Robust Control Design for Laser Cavity Squeezing in Quantum Optical Systems

Mohammad Salehizadeh

A Thesis

in

The Department

of

Electrical and Computer Engineering

Presented in Partial Fulfillment of the Requirements

for the Degree of Master of Applied Science at

Concordia University

Montréal, Québec, Canada

December 2011

CONCORDIA UNIVERSITY

SCHOOL OF GRADUATE STUDIES

This is to certify that the thesis prepared

By: Mohammad Salehizadeh

Entitled: Robust Control Design for Laser Cavity Squeezing in Quantum Optical Systems

and submitted in partial fulfilment of the requirements for the degree of

Master of Applied Science

Complies with the regulations of this University and meets the accepted standards with respect to originality and quality.

Signed by the final examining committee:

_____ Dr. Rabin Raut, Chair

_____ Dr. Ali Dolatabadi (MIE), External

_____ Dr. Xiupu Zhang , Examiner

_____ Dr. Amir G. Aghdam, Supervisor

_____ Dr. M. Zahangir Kabir, Supervisor

Approved by: _____

Dr. W. E. Lynch, Chair

Department of Electrical and Computer Engineering

_____ 2011 _____

Dr. Robin A. L. Drew

Dean, Faculty of Engineering and Computer Science

ABSTRACT

Robust Control Design for Laser Cavity Squeezing in Quantum Optical Systems

Mohammad Salehizadeh

Quantum control theory is a rapidly evolving research field, which has developed over the last three decades. Quantum optics has practical importance in quantum technology and provides a promising means of implementing quantum information and computing device. In quantum control, it is difficult to acquire information about quantum states without destroying them since microscopic quantum systems have many unique characteristics such as entanglement and coherence which do not occur in classical mechanical system. Therefore, the Lyapunov-based control methodology is used to first construct an artificial closed-loop controller and then an open-loop law is derived by simulation of the artificial closed-loop system.

This work considers the stabilization of laser cavity as the main integral part of quantum optical systems through squeezing the output beam of the cavity. As a comprehensive example of this type of system, quantum optomechanical sensors are investigated. To this end, a nonlinear model of quantum optomechanical sensors is first extended incorporating various noises. Then, linear quadratic Gaussian (LQG) control method is used to tackle the problem of mode-squeezing in optomechanical sensors. Coherent feedback quantum control is synthesized by incorporating both shot noise and back-action noise to attenuate the output noise well below the shot noise level (Two waves are said to be coherent if they have a constant

relative phase). In the second phase of this work, due to entanglement of the system with critical uncertainties and technical limitations such as laser noise and detector imprecision, robust H_∞ method is employed for the robust stabilization and robust performance of the system in practice. In H_∞ methods, a control designer expresses the control problem as a mathematical optimization problem and then finds the controller that solves this. The effectiveness of the proposed control strategy in squeezing the cavity output beam is demonstrated by simulation.

“ The more I learn, the more I learn how little I know. ” –Socrates

To my parents,

for their tireless support throughout my life

ACKNOWLEDGEMENTS

I would like to thank my supervisors Dr. Amir G. Aghdam and Dr. M. Zahangir Kabir for their sincere encouragement, guidance, and support during my Master studies.

I would also like to thank Dr. Jalal Habibi, who helped me all the time. His novel ideas and suggestions were essential for the results of this thesis; and it was a great honor for me to work with him.

I truly appreciate my family and those people who have enriched me as a professional and as a human being. I sincerely thank them because I would not be who I am without them.

This work has been supported by the Natural Sciences and Engineering Research Council of Canada (NSERC), under the Discovery Grants Program. They are really appreciated.

TABLE OF CONTENTS

LIST OF FIGURES

LIST OF TABLES

LIST OF ABBREVIATIONS AND SYMBOLS

LQG	linear quadratic Gaussian
LQR	linear quadratic regulator
QNC	quantum-noise-cancellation
PI	proportional integral
QND	quantum non-demolition
EKF	extended Kalman filter
CRDS	cavity ring-down spectroscopy
QLE	quantum Langevin equation
PBS	polarizing beamsplitters
PZT	piezoelectric transducer
LFT	linear fractional transformation

Chapter 1

Introduction

1.1 Motivation and Related Work

Quantum mechanics, also known as quantum physics or quantum theory, provides a mathematical description of the interaction of matter and energy. The theory was developed in 1925 by Werner Heisenberg [1, 2]. It describes the time evolution of physical systems via a mathematical structure called the wave function. Quantum mechanics differs significantly from classical mechanics in its predictions when the scale of observations becomes comparable to the atomic and sub-atomic scale. However, many macroscopic properties of systems can only be fully understood and explained with the use of quantum mechanics. Phenomena such as superconductivity, the properties of materials such as semiconductors and nuclear and chemical reaction mechanisms observed as macroscopic behaviour, cannot be explained using classical

mechanics [3–6].

In physics, a quantum system is said to be open if it is in interaction with an external quantum system, such as the environment. An open quantum system can be viewed as a distinguished part of a larger closed quantum system, the other part being the environment [7, 8].

Many applications involving quantum systems rely on feedback control to enhance their performance according to some practical requirements such as minimizing the control time [9, 10], the control energy [11, 12], the error between the final state and target state [13], or a combination of these. The main focus of this thesis is directed towards feedback control of a quantum optical system due to its practical importance in implementing quantum information and manufacturing computing devices [13]. In many relevant experiments, it is desired to make the laser oscillator a quantum noise-limited device [14, 15]. As a practical example, it is very important in X-ray imaging and flat-panel detectors to attenuate the quantum noise to some extent in order to improve image visualization [16]. According to the Heisenberg uncertainty principle for the quadrature components of the light field, the product of uncertainties in both components of the quadrature is greater than or equal to some quantity (introduced later) scaled by Planck's constant. Note that the uncertainty product of the amplitude and phase-noise levels even under extremely high pumping condition is typically larger than the Heisenberg minimum-uncertainty product due to the presence of nonstationary phase-diffusion noise. In order to achieve a phase-squeezed state, the pump phase fluctuation

needs to be suppressed below the ordinary shot noise level [17].

Recently, there has been increasing interest in the control of optomechanical sensors due to their wide range of applications in detecting forces, small displacements, gravitational wave interferometers, and also in quantum information cryptography [18–22]. In optics physics, in order to amplify a laser beam, a cavity is adjusted along the path of laser as it is shown in Fig. 1.1(a); this enhances the absorption path length of the beam [23, 24]. Fig. 1.1(b) illustrates the concept of laser cavity frequency locking, that is used to desirably make the spectral bandwidth of the cavity output beam narrower and lock laser frequency ω_{pump} at the resonance frequency of cavity ω_0. This generates an intense output cavity beam (note that for now the effect of mechanical frequency ω_m of micro-resonator is ignored for simplification, and will be discussed in detail in the next chapter). The nonclassical state of light (i.e., those

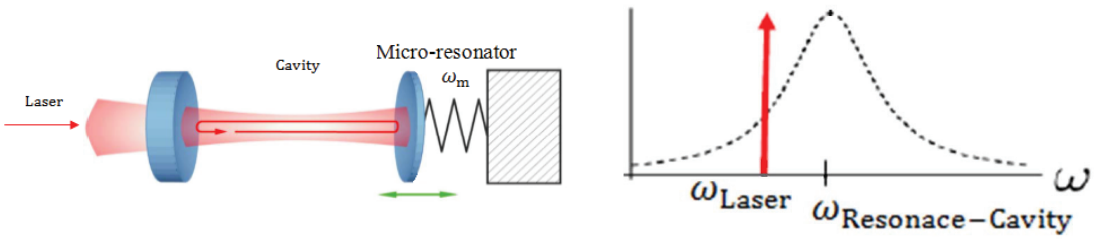

(a) (b)

Figure 1.1: (a) Schematic of optomechanical cavity, and (b) locking laser frequency at the resonance frequency of cavity to generate an intense output cavity beam.

states that have nonclassical noise properties called quantum noise, which is described based

on quantum mechanics) with a noise level below the standard quantum limit in one quadrature component is called the squeezed light. Squeezed light is best described by considering complex phasors for the representation of its state in one mode of the optical field. Due to quantum uncertainty shown by an ellipse in Fig. 1.2 (δX_a, δY_a axes show amplitude and phase quadrature states, respectively), any measurement of the complex amplitude of the light field can deliver different values within this uncertainty region. Moreover the product of the uncertainties in both components of the quadrature is greater than or equal to some quantity times Planck's constant. The objective of the present work as far as phase squeezing is concerned is to decrease the phase fluctuations of light beam, δY_a, at the expense of increased amplitude fluctuations, δX_a [25–27] (see Fig. 1.2). A variety of noise sources affect this type of sensor,

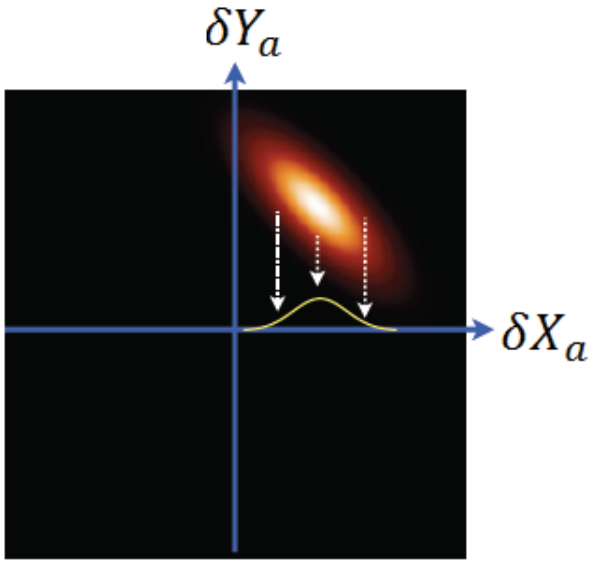

Figure 1.2: Phase-squeezed state of light, illustrated in phase diagram. The visible ellipse indicates the uncertainty region.

including shot noise which is a low-frequency noise with a relatively high amplitude. In addition to shot noise at the cavity output, quantum radiation pressure fluctuations on a moving mirror within an optical cavity can introduce excess noise, which is often referred to as the back-action noise [28]. This limits the ability to detect a classical force on the mirror [29]. To overcome this standard quantum limit and reduce the effects of various noises, it is required to squeeze the laser cavity output beam by utilizing destructive interference.

Tsang and Caves [28] proposed a scheme based on coherent feedforward quantum control by quantum-noise-cancellation (QNC), to tackle the problem of squeezing the laser cavity output beam. The method uses an ideal model for the system without considering intrinsic mechanical and optical losses and fluctuations. Vitali and Tombesi [30] employed a proportional integral (PI) feedback controller to make ponderomotive squeezing, and analyzed the overall system operation using Fourier transform. However, they did not take the effect of technical noise sources such as laser noise and electronic noise into consideration, while this type of noise is particularly not negligible in the audio band. In the presence of noise, one can take advantage of the advanced control tools to design a feedback law which minimizes the effect of noise in the output [31]. For instance, the classical Lyapunov-based control method is a powerful tool for feedback controller design. In quantum control, the acquisition of feedback information through measurements usually destroys the state being measured, which makes it difficult to directly apply the Lyapunov approach to quantum feedback control design [32–34].

Alternatively, one can first use computer simulation to find a sequence of controls. A "feedback design and open-loop control" strategy can then be adopted by applying the resultant control sequence to the quantum system in an open-loop fashion [31]. In practical applications, the realization of a quantum measurement on a quantum system is usually accomplished by entangling the system with an auxiliary probe such as homodyne detector [31].

1.2 Thesis Objectives

This work is concerned with the problem of mode-squeezing in optomechanical sensors in the presence of the dominant sources of noise which are often ignored for simplicity as discussed earlier. To this end, a linear quadratic Gaussian (LQG) controller with integral action is designed in the context of coherent feedback quantum control in order to simultaneously suppress the effects of shot noise and back-action noise while rejecting any constant disturbance applied to the system. A Fabry-Perot cavity is considered as the main integral part of an optomechanical sensor, which includes a moving mirror as a micro-resonator. The optical model of this mirror is assumed to be perfectly reflecting, and mechanically characterized as a harmonic oscillator [28]. This oscillator represents a system that, when displaced from its equilibrium position, experiences a restoring force proportional to the displacement [35]. An important contribution of this work is that it considers a more realistic setting (in terms of noise) in the model of the system, and uses an optimal control scheme to minimize the impact of all sources of noise in the output and uncertainty in the model. Also, by means of an H_∞

controller, the uncertain system is stabilized. The H_∞ control design method is based on an optimization problem which is to be solved mathematically [36]. This work is expected to pave the way for controlling the frequency of laser cavity system with fluctuations approaching the quantum noise limit, and the results can be used in a variety of applications concerning high-precision metrology and instrumentation [37].

To summarize the objectives of this project, it is aimed to employ feedback control algorithms in order to:

- Achieve frequency locking of laser cavity for the case of optomechanical sensors using optimal servo controller. To this end, an LQG controller with integral action is designed in the context of coherent feedback quantum control in order to simultaneously suppress the effects of shot noise and back-action noise, while rejecting constant disturbances.

- Improve stability and increase the measurement efficiency of a quantum optics system using a robust H_∞ controller.

1.3 Thesis Outline

This thesis is organized as follows. In Chapter 2, the basic concepts of quantum mechanics and the squeezing problem in optomechanical sensors are introduced. The nonlinear model for the system is described in Chapter 3, and is linearized subsequently. A systematic optimal control method is proposed in Chapter 4 to handle the squeezing problem in cavity. To guarantee the

stability of the system in practice, robustness analysis is carried out in Chapter 5. In each of these two chapters (4,5), the results are verified by simulations, and finally the contributions of the paper are summarized in Chapter 6.

Chapter 2

Background

This chapter provides some background information on the problem under study in this dissertation. First, basic concepts of quantum mechanics related to the present work are introduced, and then the squeezing problem in optomechanical sensors is described.

2.1 Light Propagation in a Cavity

An electromagnetic wave traveling in a medium experiences attenuation due to the fluctuation of the dipole associated by the light beam [38]. Propagation of the light beam inside a cavity is an optical parametric process, which is very sensitive to the optical phases of the waves involved. Efficient conversion usually requires phase matching to be achieved for the wavelength range of interest. The gain bandwidth is largely determined by the phase-matching bandwidth [39–41]. To this effect, the only surviving modes will have radii of curvature (R)

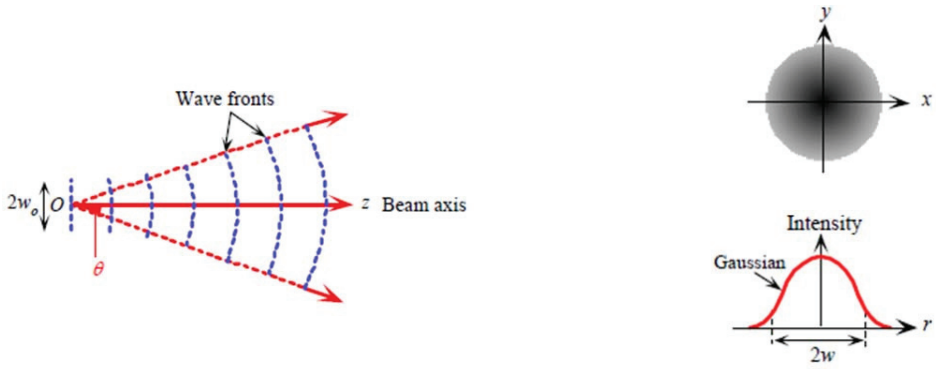

(a) (b)

Figure 2.1: (a) Wavefronts of a Gaussian light beam; (b) light intensity across beam cross section and light intensity vs. radial distance r from beam axis (z) [40].

matching that of the mirrors for a stable cavity. The light phase fronts match the mirrors. It is required to engineer the beam by choosing the mirrors, rather than choosing the mirrors to match the beam. Depending on the length of the cavity, the plane waves propagating forward and backward inside the cavity can interact constructively, resulting in stable optical modes (resonance) or destructively giving rise to unstable optical modes, as shown in Fig. 2.2. The resonance frequency of cavity is inversely related to the controlled length of the cavity L [42, 43] according to the following equation:

$$f_0 = \frac{c}{2L}(q + \frac{1}{\pi}(m+n+1)cos^{-1}\sqrt{(1-\frac{L}{\rho_1})}\sqrt{(1-\frac{L}{\rho_2})}), \tag{2.1}$$

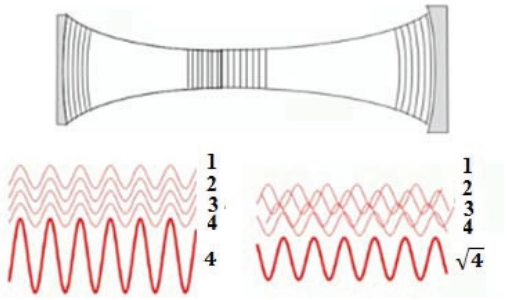

Figure 2.2: Engineering a Gaussian beam in the cavity.

where ρ_1 and ρ_2 are the radii of the two mirrors, q is the q^{th} longitudinal cavity mode being excited, c is the speed of light in vacuum, and m,n represent waveguide's modes.

2.2 Heisenberg's Uncertainty Principle

Heisenberg's uncertainty principle given below provides a fundamental limitation in quantum systems' measurements.

Theorem 2.1 *It is impossible to measure simultaneously two canonically conjugate variables such as position x and momentum p, with arbitrary precision. Furthermore,*

$$\Delta x \Delta p \geq \frac{\hbar}{2}, \tag{2.2}$$

where $\hbar$ is the reduced Plank constant and Δx and Δp are uncertainties of x and p about certain mean values.

According to Heisenberg's principle, one cannot simultaneously measure all of the variables of a system precisely. Furthermore, repeated measurements on the same system will

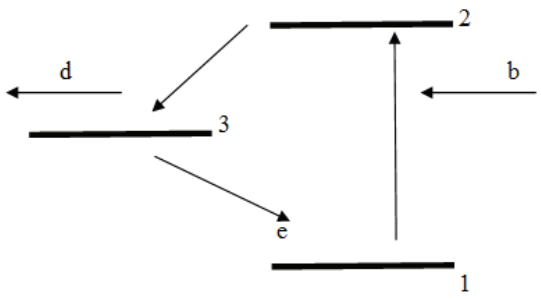

Figure 2.3: Three level atom model of a photodetector.

yield values of x and p which fluctuate about certain mean values with uncertainties Δx, Δp [44]. Due to this fundamental limit, by reducing quantum noise to zero, the mean photon number goes to infinity. This introduces a trade off between quantum noise reduction and required mean photon number, which in turn introduces a limit on the signal-to-noise ratio improvement for a fixed mean photon number. The unique feature of a squeezed state of light is that the photon-number noise can be practically reduced to zero without requiring an infinite mean photon number [17]. One of the objectives of the present work is to show that a laser oscillator can produce a phase-squeezed state, provided the pumped phase fluctuation is suppressed below the ordinary shot noise level.

2.3 Coherent State $|\alpha\rangle$

Two waves are said to be coherent if they have a constant relative phase. The degree of coherence is measured by the interference visibility. In the coherent state, the normalized correlation function of two waves is 1, which means the interference fringes of system are

maximally visible. Fig. 2.3 represents the three-level atom model of a photodetector. In this model, the photodetector process is interpreted as the individual absorption of photons with the subsequent emission of electrons. By the incident of the input mode b to a detector, electron gains enough energy to jump to the upper level. Then, according to energy continuity principle, the electron operator d with lower energy level compared to the previous one is generated as the current and the rest of energy is faded away as the lost mode e [44].

2.4 Squeezing Problem in Optomechanical Sensors

Consider an optomechanical sensor as shown in Fig. 2.4, and let the position operator, momentum operator and resonance frequency of the mirror be denoted by $q(t)$, $p(t)$ and ω_m, respectively. Let also m be the mass of the mirror (in the range of nanograms) subject to the force $f(t)$ [28, 30]. Consider an appropriate rotating reference frame, and assume the cavity is pumped with an input beam $b(t)$ with carrier frequency ω_{pump} to which all phases are referenced. Assume also that the coherent real mean amplitude of the beam, represented by $< b(t) >$, is denoted by β. The intracavity destructive optical field $a(t)$ decays due to coupling (through the partially transmitting mirror) to the output beam $b_{out}(t)$. Let the rate of decay of $a(t)$ be denoted by κ. The parameter b_1 is the transmitted mode and b_L is the loss mode. In particular, the above-mentioned operators have the canonical commutation properties $[q(t), p(t)] = i\hbar$, $[a(t), a^*(t)] = 1$, and $[b(t), b^*(t^{'})] = \delta(t - t^{'})$, where the asterisk represents the complex conjugate of the operator [28]. Using the amplitude and phase quadrature

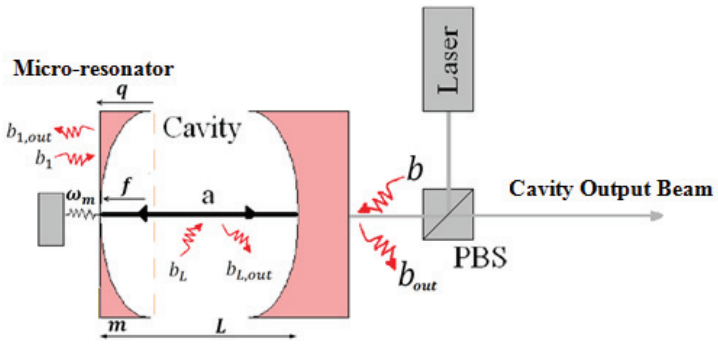

Figure 2.4: Description of operators in the optomechanical cavity.

operators, one can write:

$$b = \beta + (X_{b_0} + iY_{b_0})/\sqrt{2}, \tag{2.3a}$$

$$b_{out} = \beta + (\eta_1 + i\eta_2)/\sqrt{2}, \tag{2.3b}$$

$$a = \alpha + (\delta X_a + i\delta Y_a)/\sqrt{2}. \tag{2.3c}$$

The system is linearized about the zero-detuning point. In the linearized model, the output signals can be represented as the sum of independent contributions from the reference input signal and noise (from the principle of superposition). As such, Fig. 2.5 depicts the input-output flow diagram of the cavity. In this figure, G represents the optomechanical coupling factor [30]. The effect of the input amplitude fluctuation X_{b_0} on the output phase quadrature η_2 is commonly known as back-action noise which is due to the Kerr-like ponderomotive coupling of the cavity amplitude quadrature δX_a to the phase quadrature δY_a [28]. The effect

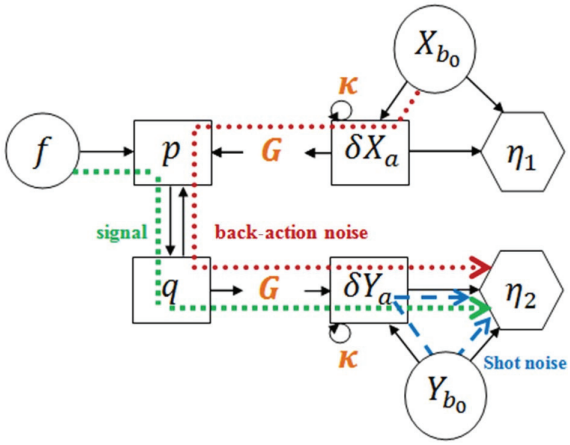

Figure 2.5: Input-output flow diagram of cavity in optomechanical sensors.

of the input phase fluctuation Y_{b_0} on the output phase quadrature η_2, on the other hand, is modeled as an undesirable signal called the shot noise. The discrepancy between the laser frequency and the resonance frequency of the cavity is referred to as the *detuning variable* and is denoted by Δ_0. In the presence of the radiation pressure interaction of the cavity mode with a vibrating resonator, the detuning variable is defined as $\Delta_0 = \omega_{pump} - \omega_0$, and the effective detuning variable is given by $\Delta = \Delta_0 - |\alpha|^2 \sum_j \frac{(G_0^j)^2}{\omega_j}$. Here ω_0 is the resonance frequency of the cavity when the interaction of laser beam with the micro-resonator is neglected, α denotes the steady-state average of the intracavity operator a when Δ approaches zero, and ω_j is the set of harmonics that the micro-resonator produces after the incident of photons. Consider now a one-dimensional case, where the light is sensitive only to mirror surface deformations along the cavity axis. In this case, ω_m represents the resonance frequency of the micro-resonator instead of a set of harmonic excitations [30]. Depending on the magnitude of the effective detuning variable, three cases of special interest are as follows [45]:

i) $\Delta = +\omega_m$: cooling

ii) $\Delta = 0$: quantum non-demolition (QND)

iii) $\Delta = -\omega_m$: entanglement

The objective is to make the cavity output beam ponderomotive squeezing. In other words, it is desired to generate a phase quadrature squeezed light at the cavity output in the presence of back-action noise and shot noise predominantly, which is detectable from the phase quadrature measured by the homodyne detector.

In Fig. 2.6, the effective frequency of cavity is modified as $\omega_{cavity} = \omega_0 \pm \omega_m$ due to the back-action noise, i.e., the static radiation pressure of incident photons on the moving mirror. In fact, this figure represents the QND case to eliminate the effect of back-action noise by locking three spectral peaks on the left axis onto one resonance frequency on the right axis. This in turn drives Δ to zero in the squeezed state by changing the effective length of the cavity. The micro-resonator (as a part of the cavity) is shifted proportionally to the intracavity intensity, and therefore provides the capability of highly precise measurements in squeezed state regime. Moreover, it can be verified that stability in the case of resonance is much easier to be checked compared to the off-resonance case [30] and for the squeezing detection, one needs to tune and stabilize the phase of the homodyne detector, which can be realized systematically by means of a proper feedback controller.

The above-mentioned problem has been investigated in the physics community for a number of years, and is known to be a difficult problem because of an almost complete loss

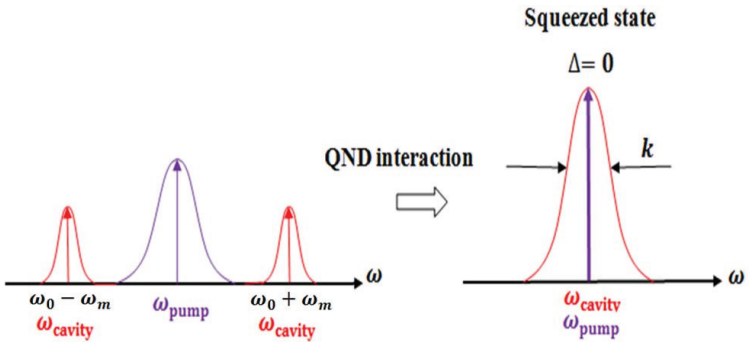

Figure 2.6: Eliminating the effect of back-action noise by properly shifting three spectral peaks.

of observability when the system goes out of lock into the nonlinear region [46]. Frequency locking of the optical cavity has many applications. For instance, recently, Boyson et al. in [47] considered the application of a discrete-time extended Kalman filter (EKF) to the problem of estimating the ring-down time constant of a Fabry-Perot optical cavity for the purpose of cavity ring-down spectroscopy (CRDS). The ring-down time corresponds to the time it takes for the light inside an optical cavity to decay to $1/e$ ($e^{-1} = 0.368$) times its initial intensity. The online estimation of the ring-down time (or decay time) for a cavity is a direct indication of the absorbing species contained in it and can be used to detect improvised explosive devices and concealed explosives [48].

Chapter 3

System Model

In this chapter, a comprehensive schematic of optomechanical sensors is presented, then a basic nonlinear model for the particular case of optomechanical sensors is extended. The material of the following two chapters are mainly extracted from [49].

3.1 Complete Model

Fig. 3.1 shows the block diagram of the cavity optomechanical system integrated with a homodyne detector. Once the measured phase quadrature signal passes through the controller loop onto a piezoelectric, the actuator stimulates the destructive effect into the intracavity light fluctuations by manipulating over the moving mirror. The cavity consists of two mirrors: one is relatively massive and the other one is very high-finesse and light weight [50]. It is recommended to choose a high-quality mechanical resonator to suppress thermal noise

disturbance. Given the laser input beam b, the parameter b_1 is the transmitted mode, b_L is the loss mode, and b_{out} is the output mode measured using homodyne detector [46]. Moreover, ϕ_{LO} is the relative phase shift between the output mode b_{out} and the local oscillator mode [51]. The beamsplitters shown in the figure have a balanced 50/50 reflectivity. The transfer function $H(s)$ represents the feedback control law which includes an integrator as discussed later. The figure also shows that in the two-port homodyne detector the intensities from both output ports of a 50-50 beamsplitter are monitored through the two photodiodes D_1 and D_2, subtracting the two outputs and retaining only the interference terms. The laser system which is used in this work is pumped by approximately 30mW of the 1.064μm, single-mode output of a diode-laser, miniature monolithic Nd:YAG laser used as the input to a linear cavity [13].

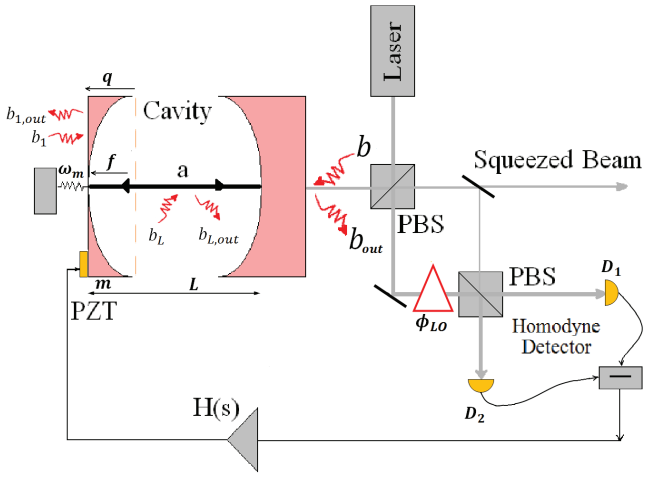

Figure 3.1: Schematic view of an optomechanical system with a homodyne-based feedback control applied to the micro-resonator (moving mirror). Note: PBS and PZT in the figure stand for polarizing beamsplitters and piezoelectric transducer, respectively.

3.1.1 Nonlinear quantum Langevin description of the optomechanical system

The cavity in this type of system can be described by quantum Langevin stochastic differential equations based on Heisenberg principle in rotational frame at the laser frequency ω_{pump} as follows [30]:

$$\dot{q}_j = \omega_j p_j, \tag{3.1a}$$

$$\dot{p}_j = -\omega_j q_j - \gamma_j p_j + G_0^j a^* a + \ddot{\xi}, \tag{3.1b}$$

$$\dot{a} = -(\kappa + i\Delta_0)a - i\sum_j G_0^j a q_j + E + \sqrt{2\kappa_0} b_0 + \sqrt{2\kappa_1} b_1 + \sqrt{2\kappa_L} b_L, \tag{3.1c}$$

$$b_{out} = \sqrt{2\kappa_0} a - b_0. \tag{3.1d}$$

It is important to note that the product $\Delta_0 a$ in (3.1c) introduces nonlinearity in the equation. Also, $\kappa = \kappa_0 + \kappa_1 + \kappa_L$, where $\kappa_0, \kappa_1, \kappa_L$ are the decay rates of the corresponding optical fields b_0, b_1 and b_L [13]. Moreover, $\ddot{\xi}$ is the acceleration enforced by the actuator on the micro-resonator which will be discussed later in detail. The motion of the micro-resonator can be described by the vibrational normal modes, each with its own resonance frequency ω_j and damping rate $\gamma_j = \frac{\omega j}{Q_0}$, where Q_0 is the cavity quality factor [30]. The parameter E is related

to the input power P_{in} and is expressed as:

$$E = \sqrt{2P_{in}\kappa/\hbar\omega_{pump}}\,. \tag{3.2}$$

Note that G_0^j in (3.1b) and (3.1c) represents the optomechanical couplings that is given by:

$$G_0^j = \frac{\omega_{pump}c}{L}\sqrt{\frac{\hbar}{m_j\omega_j}}, \tag{3.3}$$

where c is the speed of light and L is the length of the cavity. Under the assumption that the driving laser and cavity are perfectly aligned, light is sensitive only to the mirror surface deformations along the cavity axis (one degree of freedom). Hence, one can simply consider ω_m as the single resonance frequency of the micro-resonator and get rid of the index j in the equations, accordingly [30].

3.1.2 Linearization

In order to design the linear quadratic Gaussian (LQG) controller for the system, the nonlinear equations pertinent to the optical subsystem need to be linearized first. It is assumed that the conditional state associated with the underlying quantum system is formulated in such a way that a linearized model of the system can be derived as a “good" approximation of it in a sufficiently small region around the operating point. The standard linearization method is applied by considering small variation of the corresponding variables around their steady-state

coherent values as:

$$a = \alpha + \delta a, \tag{3.4a}$$

$$q = q_s + \delta q, \tag{3.4b}$$

$$p = p_s + \delta p. \tag{3.4c}$$

On the other hand, the cavity destructive operator is related to the amplitude and phase quadratures as follows [13, 52]:

$$\delta X_a = \frac{\delta a + \delta a^*}{\sqrt{2}}; \quad \delta Y_a = \frac{\delta a - \delta a^*}{i\sqrt{2}}. \tag{3.5}$$

Similarly, the quadrature of the input and noise fields are given by:

$$X_{bj} = \frac{b_j + {b_j}^*}{\sqrt{2}}; \quad Y_{bj} = \frac{b_j - {b_j}^*}{i\sqrt{2}}; \quad j = 0, 1, L. \tag{3.6}$$

The following expressions provide the equilibrium point around which the nonlinear algebraic equations are linearized [30]:

$$\alpha = \frac{E}{\kappa + i\Delta}, \tag{3.7a}$$

$$q_s = \frac{G_0|\alpha|^2}{\omega_m}, \tag{3.7b}$$

$$p_s = 0, \tag{3.7c}$$

where Δ is the effective detuning introduced earlier. Note that nonlinear terms like $\delta a^* \delta a$ and $\delta a \delta q$ [30] have been ignored without loss of generality, and the term of $\delta a q$ has been enclosed as effective Δ. Now, to solve this nonlinearity, let α denote the steady-state average of a when $\Delta = 0$, so that $0 = -\kappa\alpha + \sqrt{2\kappa_0}\beta$, and hence $\alpha = \frac{\sqrt{2\kappa_0}}{\kappa}\beta$, which is a real number [13]. The linearized model can then be obtained as:

$$\begin{aligned}
\delta\dot{q} &= \omega_m \delta p, && \text{(3.8a)}\\
\delta\dot{p} &= -\omega_m \delta q - \gamma_m \delta p + G\delta X_a + \ddot{\xi}, && \text{(3.8b)}\\
\delta\dot{X}_a &= -\kappa\delta X_a + \sqrt{2\kappa_0} X_{b_0} + \sqrt{2\kappa_1} X_{b_1} \\
&\quad + \sqrt{2\kappa_L} X_{b_L}, && \text{(3.8c)}\\
\delta\dot{Y}_a &= -\kappa\delta Y_a + 2\alpha\Delta + G\delta q + \sqrt{2\kappa_0} Y_{b_0} \\
&\quad + \sqrt{2\kappa_1} Y_{b_1} + \sqrt{2\kappa_L} Y_{b_L}. && \text{(3.8d)}
\end{aligned}$$

Here G is defined as the effective optomechanical coupling and is equal to $G_0\alpha\sqrt{2}$. The output of the homodyne detector shown in Fig. 3.1 is the so-called rotated-field quadrature operator given by [44, 53]:

$$X_{\phi_{LO}} = \frac{e^{j\phi_{LO}} a^* + e^{-j\phi_{LO}} a}{\sqrt{2}} = \delta X_a cos(\phi_{LO}) + \delta Y_a sin(\phi_{LO}), \qquad (3.9)$$

where ϕ_{LO} is the phase of the local oscillator. On the other hand:

$$y = k_2\sqrt{2\kappa_0}(\delta X_a cos(\phi_{LO}) + \delta Y_a sin(\phi_{LO})) - k_2 X_{b_0} + \varepsilon_3 w_3, \tag{3.10}$$

where k_2 denotes the transimpedance gain of the homodyne detector. The sensor measurement noise $\varepsilon_3\omega_3$ is assumed to be a white Gaussian noise process with variance ${\varepsilon_3}^2$ [13].

3.1.3 Shot noise model

In essence, shot noise (which is sometimes referred to as laser phase noise) is characterized by its low-frequency and high amplitude. It can be modeled as a low-pass disturbance whose Laplace transform has a pole located at ε_4 and has a constant gain k_s, i.e.:

$$\dot{\xi}_s = -\varepsilon_4\xi_s + w_s; \quad w_2 = k_s\xi_s, \tag{3.11}$$

where w_s is white Gaussian noise and w_2 is shot noise [54].

3.1.4 Piezoelectric actuator model

The piezoelectric actuator model that is used here is the same as the one introduced in [54] expressed as:

$$\ddot{\xi} + r_1\dot{\xi} + r_2\xi = u + w_1, \tag{3.12a}$$

$$\Delta = c_1\dot{\xi} + c_2\xi + w_2 + Osp. \tag{3.12b}$$

Mechanical noise w_1 in (3.12a) is white Gaussian noise with variance ${\varepsilon_1}^2$, which is treated as a design parameter. Furthermore, Osp in (3.12b) is, in fact, an offset parameter which is caused by the static radiation pressure of photons.

3.1.5 State-space representation

In order to design an LQG controller for this system, the combined state-space model of the actuator, plant and measurement sensor is required, which is expressed as:

$$\begin{aligned} \dot{x} &= Ax + Bu + D_1 w, \\ y &= Cx + D_2 w. \end{aligned} \tag{3.13}$$

As for the optomechanical subsystem (which contains the dynamics of both optical and micro-resonator components), one can write:

$$\begin{bmatrix} \delta\dot{X}_a \\ \delta\dot{Y}_a \\ \delta\dot{q} \\ \delta\dot{p} \end{bmatrix} = \begin{bmatrix} -\kappa & 0 & 0 & 0 \\ 0 & -\kappa & G & 0 \\ 0 & 0 & 0 & \omega_m \\ G & 0 & -\omega_m & -\gamma_m \end{bmatrix} \begin{bmatrix} \delta X_a \\ \delta Y_a \\ \delta q \\ \delta p \end{bmatrix} + \begin{bmatrix} 0 \\ 2\alpha \\ 0 \\ 0 \end{bmatrix} \Delta + \sqrt{2\kappa_0} \begin{bmatrix} cos\phi_{LO} & sin\phi_{LO} \\ -sin\phi_{LO} & cos\phi_{LO} \\ 0 & 0 \\ 0 & 0 \end{bmatrix} \begin{bmatrix} X_{b_0} \\ Y_{b_0} \end{bmatrix}$$
$$+ \sqrt{2\kappa_1} \begin{bmatrix} 1 & 0 \\ 0 & 1 \\ 0 & 0 \\ 0 & 0 \end{bmatrix} \begin{bmatrix} X_{b_1} \\ Y_{b_1} \end{bmatrix} + \sqrt{2\kappa_L} \begin{bmatrix} 1 & 0 \\ 0 & 1 \\ 0 & 0 \\ 0 & 0 \end{bmatrix} \begin{bmatrix} X_{b_L} \\ Y_{b_L} \end{bmatrix} + \begin{bmatrix} 0 \\ 0 \\ 0 \\ 1 \end{bmatrix} \ddot{\xi}. \tag{3.14}$$

The homodyne detector output y can then be expressed as:

$$y = k_2\sqrt{2\kappa_0} \begin{bmatrix} cos\phi_{LO} & sin\phi_{LO} & 0 & 0 \end{bmatrix} \begin{bmatrix} \delta X_a \\ \delta Y_a \\ \delta q \\ \delta p \end{bmatrix} - k_2 \begin{bmatrix} 1 & 0 \end{bmatrix} \begin{bmatrix} X_{b_0} \\ Y_{b_0} \end{bmatrix} + \varepsilon_3 w_3. \tag{3.15}$$

The state-space representation of the piezoelectric, on the other hand, is:

$$\begin{bmatrix} \dot{\xi}_1 \\ \dot{\xi}_2 \end{bmatrix} = \begin{bmatrix} 0 & 1 \\ -r_2 & -r_1 \end{bmatrix} \begin{bmatrix} \xi_1 \\ \xi_2 \end{bmatrix} + \begin{bmatrix} 0 & 0 \\ 1 & 0 \end{bmatrix} \begin{bmatrix} w_1 \\ w_2 \end{bmatrix} + \begin{bmatrix} 0 \\ 1 \end{bmatrix} u, \tag{3.16}$$

$$\Delta = \begin{bmatrix} c_2 & c_1 \end{bmatrix} \begin{bmatrix} \xi_1 \\ \xi_2 \end{bmatrix} + \begin{bmatrix} 0 & 1 \end{bmatrix} \begin{bmatrix} w_1 \\ w_2 \end{bmatrix} + Osp. \tag{3.17}$$

As shown in Fig. 3.2, the effective detuning variable Δ is a result of the following three phenomena: cavity mirror movement by PZT, laser phase shot noise, and an offset parameter due to back-action noise (as discussed earlier), given by $Osp = -|\alpha|^2 \frac{G_0^2}{\omega_m}$.

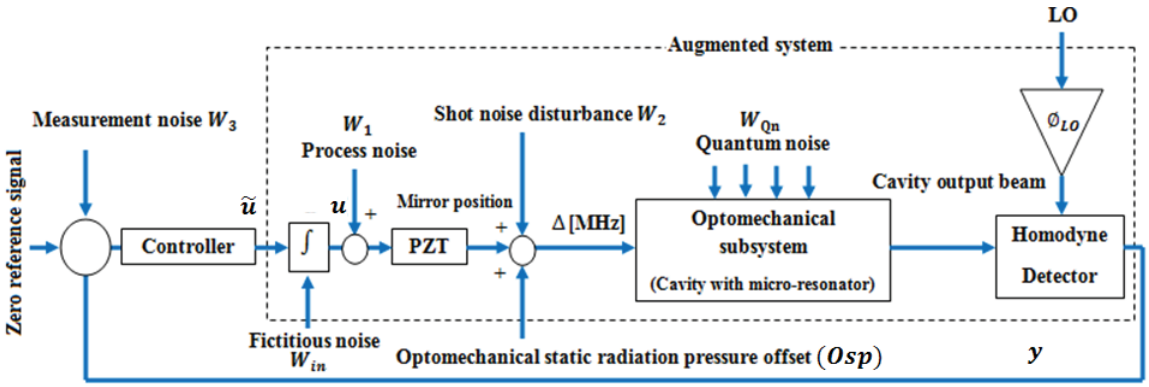

Figure 3.2: Block diagram of the closed-loop system with all sources of noise.

3.2 System Properties

3.2.1 Open-loop poles and zeros

In summary, the augmented system has eight states as follows:

- Four optomechanical states including:
  - Two states as the amplitude and phase optical quadratures,
  - Two states as the position and momentum of the micro-resonator.
- Two states as the position and momentum of the piezoelectric actuator.
- One state as the shot noise cut-off frequency.
- One state as the integrator.

Given the values of parameters in Table 3.1, one can compute various characteristics of the system. As it is evident from Table 3.2, since the value of optomechanical coupling G_0 is much smaller than the value of optical coupling κ, a pair of zeros have location very close to a pair of ploes at s-plane. Also, the existence of a positive zero is leading to the non-minimum phase behavior of the system. Obviously, two poles are omitted by the same zeros as it was expecting, since typically $\phi = \frac{\pi}{2}$ then the quadrature δX_a has no effect on the pole-zero characteristic; Also, shot noise pole arrangement in the state-space realization is kind of isolated eigenvalue. Apparently, the significant order difference which exists between the

Table 3.1: Model parameters used in simulations.

Model Parameter	Value	Unit
κ	1×10^6	rad/s
κ_0	6×10^5	rad/s
κ_1	3×10^5	rad/s
κ_L	1×10^5	rad/s
ϕ_{LO}	$\pi/2$	rad
k_2	1×10^{-5}	V/MHz
m	1×10^2	ng
L	6	cm
f_m	$200 - 600$	KHz
γ	20	Hz
β	7×10^7	Hz
Q_0 (at $T = 4K$)	1×10^4	-
G_0	$0.1 - 10$	-
r_1	958.4	-
r_2	4.25×10^8	-
c_1	-4.48×10^3	-
c_2	8.86×10^8	-
k_s	1×10^6	-
ε_4	1×10^{-3}	-
R	1×10^{-5}	-

Table 3.2: Location of poles and zeros.

Poles $\times 10^3$	Zeros $\times 10^3$
-1000	$-0.00926 + 200.01i$
$-0.479 + 20.61i$	$-0.00926 - 200.01i$
$-0.479 - 20.61i$	197.769
$-0.01 + 200i$	-0.000001
$-0.01 - 200i$	-1000
-1000	–
-0.000001	–
0	–

maximum and the minimum eigenvalue will result in having a high condition number for the system.

3.2.2 Controllability and stabilizability

The system has a transfer function from control input $\tilde{u}$ to output y as follows (see Fig. 3.2):

$$\frac{-752640(s-1.978e005)(s^2+18.53s+4e010)}{s(s+1e006)(s^2+958.4s+4.25e008)(s^2+20s+4e010)}, \tag{3.18}$$

The system is not controllable since it is not full rank (rank equals to 2).

Remark 3.1 *(Necessity condition): For a linear-fractional transformation, based on internal model theorem, an internally stabilizing controller exists if the plant system is stabilizable and detectable [55, 56].*

Stabilizability and detectability of the system were confirmed through computing the canonical form of the augmented system. Hence, it satisfies the necessity condition needed for using state feedback controller based on Remark 3.1. Having a variety of time varying parameters in the systems, the choice of classical controller such as PID does not seem to be successful in the sense of poor robustness and required bandwidth characteristics. Laser cavity as a quantum system due to some complexities such as nonlinearity, wide range of signal variations, slow and fast dynamics (system level), non-minimum phase behavior, and noise source requires to be controlled in a systematic way which can be quiet well complied

using feedback controller. Furthermore, it provides us this opportunities to [13]:

- Globally define the optimal performance of the controlled system when there are multiple design objectives.
- Incorporate the physical constraints of the plant, measurement and controller into the optimal design.

3.3 Summary

In summary, in this chapter a comprehensive nonlinear model for the case of optomechanical sensors is extended incorporating various fundamental noises. Moreover, in order to benefit from linear optimal controller, the nonlinear model is linearized around the equilibrium point. Afterwards, controllability and stabilizability status of the system are investigated. Although the system is not controllable, it holds the necessity conditions of stabilizability and detectability needed for using state feedback controller. According to the inherent aspect of a quantum system that states of the system are not directly measurable, an observer with an excellent performance as Kalman filter is necessary to observe the states of the system coupled by linear quadratic regulator (LQR) as state feedback controller. The series of Kalman filter and LQR is called LQG controller which will be discussed extensively in the next chapter.

Chapter 4

Controller design

In the current chapter, linear quadratic Gaussian (LQG) control method is used to tackle the problem of mode-squeezing in optomechanical sensors. Coherent feedback quantum control is synthesized by incorporating both shot noise and back-action noise to diminish the output noise well below the shot noise limit. The effectiveness of the proposed control strategy in squeezing the cavity output beam is demonstrated by simulation.

4.1 LQG Controller Design with Integral Action

In the design of servo controllers, it is often required to include integral action to offset constant disturbances and track constant references [57]. The optomechanical systems, on the other hand, are subject to large initial DC offset and slowly varying disturbances in addition to shot noise and back-action static radiation. Hence, an integrator is required in the forward path

as part of the servo-compensator. An LQG controller, however, does not include an integral action. Therefore, an augmented system consisting of the plant and an integrator is considered first, and the LQG controller is subsequently designed for the augmented system. The overall controller for the original plant is, in fact, the resultant LQG controller followed by an integrator. The state-space matrices for the augmented system described above can be derived from (3.13) as (see Fig. 4.1):

$$\tilde{A} = \begin{bmatrix} A & B \\ 0 & 0 \end{bmatrix}; \qquad \tilde{B} = \begin{bmatrix} 0 & 0 & 0 & 0 & 0 & 0 & 0 & 1 \end{bmatrix}';$$
$$\tilde{C} = \begin{bmatrix} C & 0 \end{bmatrix}; \qquad \tilde{D} = 0 \tag{4.1}$$

with the following augmented state and noise vectors:

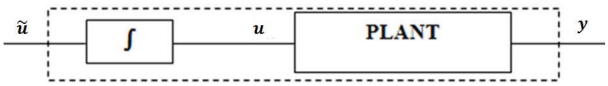

Figure 4.1: Augmented system structure including the plant and an integrator.

$$\tilde{x} = \begin{bmatrix} \delta X_a & \delta Y_a & \delta q & \delta p & \xi_1 & \xi_2 & \xi_s & \xi_{in} \end{bmatrix}, \tag{4.2}$$

$$w = \begin{bmatrix} X_{b_0} & Y_{b_0} & X_{b_1} & Y_{b_1} & X_{b_L} & Y_{b_L} & w_1 & w_3 & w_s & w_{in} \end{bmatrix} \tag{4.3}$$

where ξ_{in} and w_{in} are the integrator state and fictitious input white Gaussian noise, respectively.

The control target is to maximize the phase quadrature squeezing by minimizing the cavity detuning Δ, which is not available for measurement. The controller is designed in such a way that not only does it minimize Δ as a linear combination of the state variables, but it also regulates the output signal as noted in the previous paragraph. The reason is that based on equation (3.1), in the special case of optomechanical application the effect of back-action noise is not negligible, and minimizing variations in Δ does not guarantee minimum variations in y, and vice versa. To this end, the following cost function is considered:

$$J = \lim_{T\to\infty} \mathbf{E}\Big\{ \frac{1}{T} \int_0^T [\, \tilde{x}^T Q\, \tilde{x} + \tilde{u}^T R\, \tilde{u}\,]\, dt \Big\} \tag{4.4}$$

where the symmetric weighting matrices $Q \geq 0$ and $R > 0$ are typically chosen in such a way that the maximum contributions of the two terms in the above integral are balanced.

In order to suppress the effective detuning variable Δ, it is important to take into account the offset signal resulted from the static radiation pressure of photons incident on the micro-resonator. A Kalman filter is designed to minimize the effect of all sources of noise in the output. The structure of this filter is shown in Fig. 4.2, with the inputs $\tilde{u}$, y, Osp and the output $\hat{\tilde{x}}$ as the optimal estimated state of the augmented system. It is known that [58]:

$$\tilde{u} = F\hat{\tilde{x}}, \tag{4.5}$$

with $F = -R^{-1}\tilde{B}^T S$, where S satisfies the following algebraic Riccati equation:

$$0 = S\tilde{A} + \tilde{A}^T S + Q - R^{-1} S\tilde{B}^T \tilde{B} S. \tag{4.6}$$

Here $\hat{\tilde{x}}$ is obtained from the following equation:

$$\dot{\hat{\tilde{x}}} = \tilde{A}\hat{\tilde{x}} + \tilde{B}\tilde{u} + L[y - \tilde{C}\hat{\tilde{x}}] + Osp. \tag{4.7}$$

The steady-state Kalman filter is obtained by choosing the gain matrix L as:

$$L = P\tilde{C}TV_2^{-1}, \tag{4.8}$$

where P is the solution of the matrix Riccati equation:

$$0 = \tilde{A}P + P\tilde{A}^T + V_1 - P\tilde{C}^T V_2^{-1}\tilde{C}P. \tag{4.9}$$

The covariances of the uncorrelated process and measurement noise are respectively given by:

$$V_1 = D_1 \,\mathrm{diag}[\varepsilon_{Qn}^2, \varepsilon_{Qn}^2, \varepsilon_{Qn}^2, \varepsilon_{Qn}^2, \varepsilon_{Qn}^2, \varepsilon_{Qn}^2, \varepsilon_1^2, \varepsilon_3^2, \varepsilon_s^2, \varepsilon_{in}^2] D_1^T, \tag{4.10}$$

and

$$V_2 = \varepsilon_3^2 \tag{4.11}$$

where $\varepsilon_3^2 = \mathrm{E}[w_3 w_3^T]$. In the simulations of the next section, the quantum noise variances were chosen uniformly as $\varepsilon_{Qn}^2 = \varepsilon_s^2 = 1$; the mechanical noise variance $\varepsilon_1^2 = 10^{-4}$; the integral fictitious noise variance $\varepsilon_{in}^2 = 10^{-8}$, and the measurement noise variance $\varepsilon_3^2 = 25$ (These variances are chosen in accordance to [30], [54]).

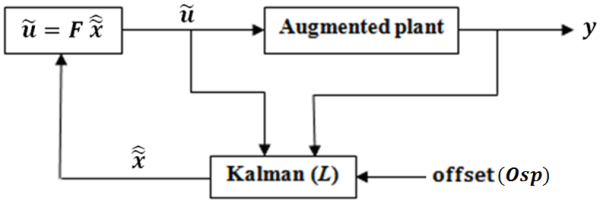

Figure 4.2: The closed-loop structure of the system with the Kalman filter.

4.2 Simulations

The simulation parameters used in this section are the same as the ones in [30], [54], and the noise models are specifically chosen to be compatible with the experimental conditions. These models are in accordance with the results by Yamamoto et al. [17] that the freely propagating output of any feedback loop based on a beamsplitter must have a noise power level greater than the quantum noise limit. In particular, for $\varepsilon_{QNL} = 1$ considered here, $\varepsilon_{Measurement} = \varepsilon_3 = 5$ which is greater than 1.

To achieve ponderomotive squeezing in the presence of various noises, one requires a strong radiation pressure interaction. This in turn is achieved when the intracavity field is very

intense. The laser system is pumped by approximately 30mW input power of single-mode output from a diode-laser with a central wavelength of 1.064μm.

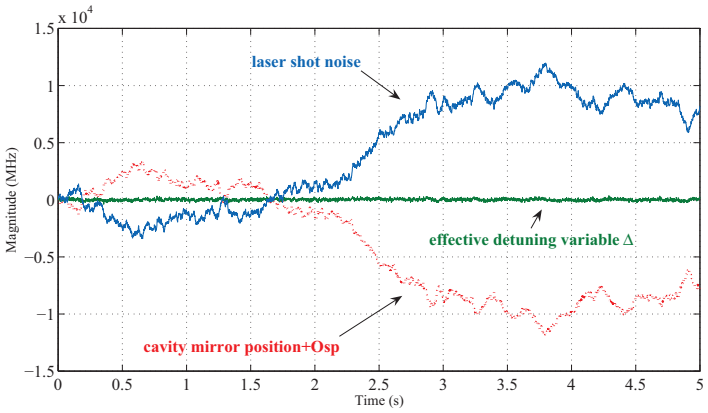

Figure 4.3: The effective detuning variable Δ along with its components for $f_m = 200$KHz.

Simulations are performed on MATLAB Simulink environment using the block diagram of Fig. 3.2 with the model parameters provided in Table 3.1. Different vibrational modes are considered in the frequency range $200\text{KHz} \leq f_m \leq 600\text{KHz}$. Fig. 4.3 illustrates the time history of the effective detuning variable Δ for $f_m = 200$KHz under the proposed controller. The output of the system is provided with and without controller in Fig. 4.4. One can observe from Figs. 4.3 and 4.4 that under the proposed controller (consisting of the integrating linear quadratic regulator (LQR) and the Kalman filter) the effective detuning variable Δ and output y are both regulated well below the shot noise level. Fig. 4.5 depicts the effective detuning variable for an open-loop laser system that is unstable, as noted earlier. Obviously, micro-resonator movement cannot conform with the existing laser noises, and hence the detuning variable curvature is very close to the shot noise curvature instead of being suppressed around

zero (which is desirable). Under the proposed LQG controller, the system is robust to the external disturbances and can reject (to a great extent) the effect of noises. To verify this by simulation, a constant disturbance of magnitude 10V is imported at the point where zero reference input signal is placed in Fig. 3.2 (note that the magnitude of disturbance signal needs to be chosen relatively larger than the quantum noise amplitude which is typically around 0.1V). As demonstrated in Fig. 4.6, the output signal y rapidly settles down to its steady-state value. From these simulations, it can be concluded that an LQG controller is very effective in reducing the effect of different sources of noise, and in particular the effect of shot noise and back-action noise, simultaneously.

It is important to note that thus far the linearized model has been used in the simulations. This is the same model used to design the controller. For more realistic simulations, however, one should use the designed controller with the original nonlinear model. Figs. 4.7 and 4.8 present the simulations with the original nonlinear model, analogous to Figs. 4.3 and 4.4. The results show that the regulation objective is achieved with the nonlinear model as well.

The Bode diagram of the proposed controller is depicted in Fig. 4.9, which shows low magnitude in low frequencies to suppress the effect of shot noise which (unlike typical noise characteristics) has high magnitude in low frequencies and almost flat magnitude in higher frequencies. This is a desirable characteristic of the controller. As it is obvious in Fig. 4.10, Kalman filter has been able to properly estimate the shot noise state in the nonlinear system using the proposed controller.

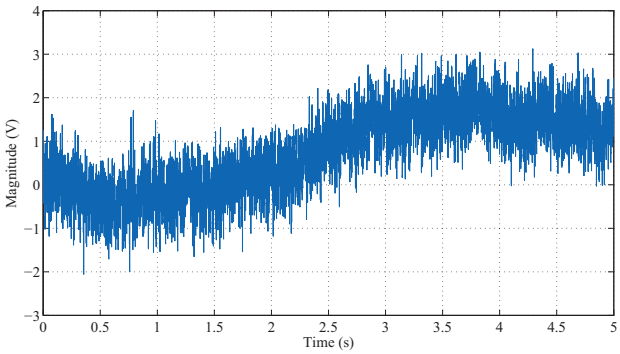

(a)

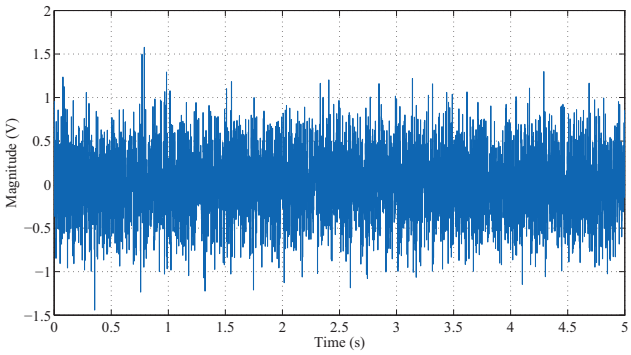

(b)

Figure 4.4: Comparison of the homodyne detector output signal y for $f_m = 200$KHz (a) without controller, and (b) with the proposed LQG controller.

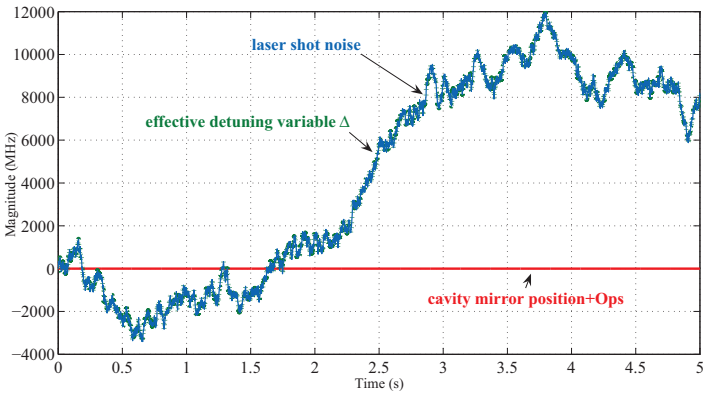

Figure 4.5: Characteristics of Δ for an open-loop laser system (with no controller).

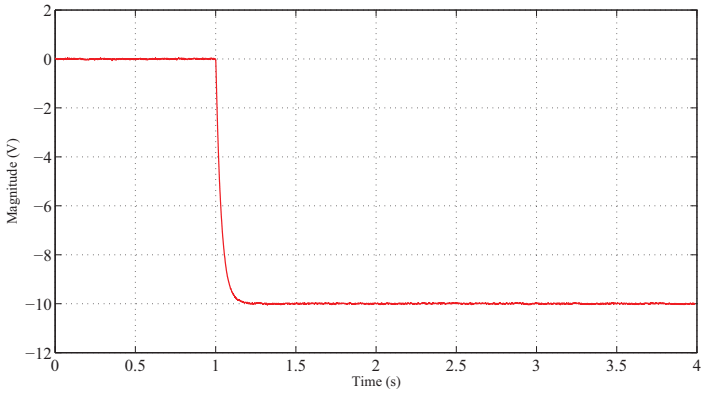

Figure 4.6: Step response of the closed-loop laser system to a step disturbance input of magnitude 10V, where the change in the magnitude of the signal occurs at $t = 1$s.

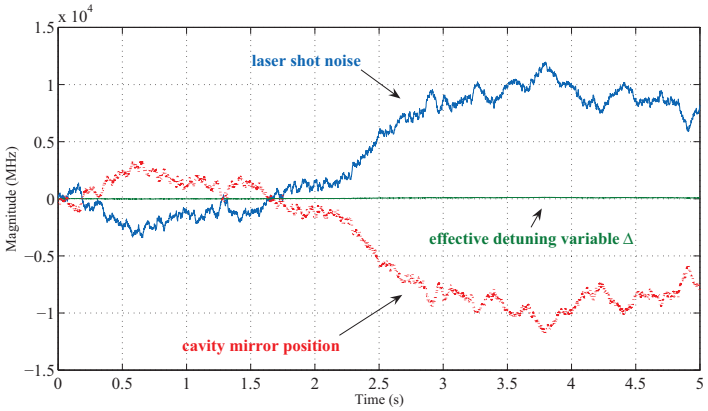

Figure 4.7: The effective detuning variable Δ along with its components for $f_m = 200$KHz obtained by using the nonlinear model.

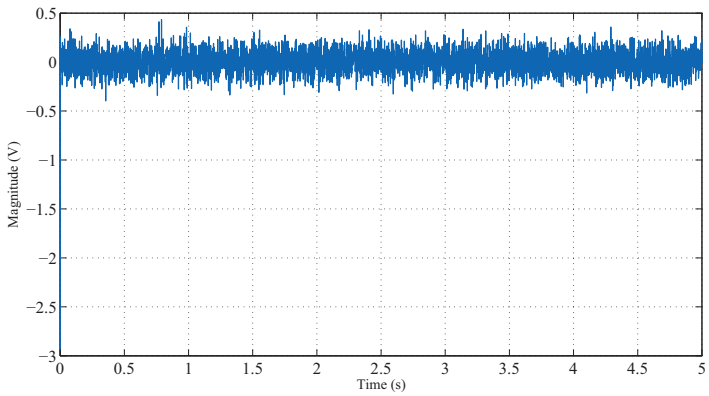

Figure 4.8: Homodyne detector output signal y obtained by using the nonlinear model with the proposed LQG controller.

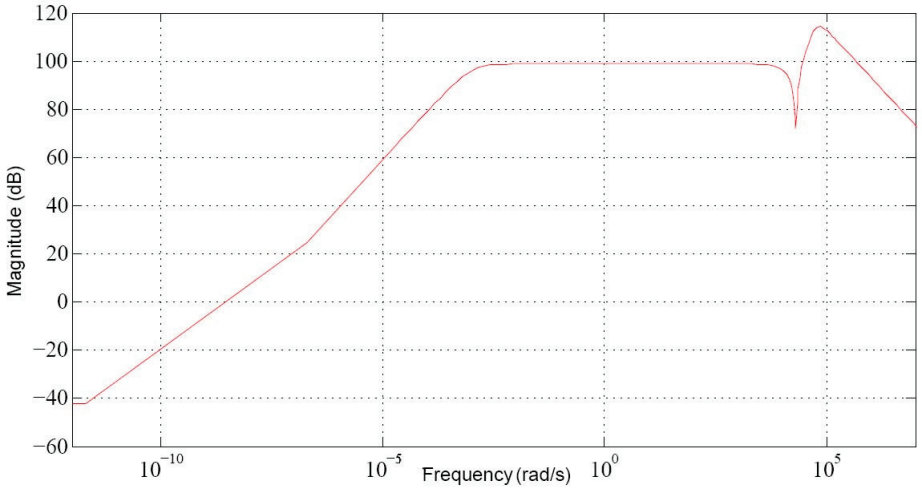

Figure 4.9: Bode diagram of the designed controller from output y to input $\tilde{u}$.

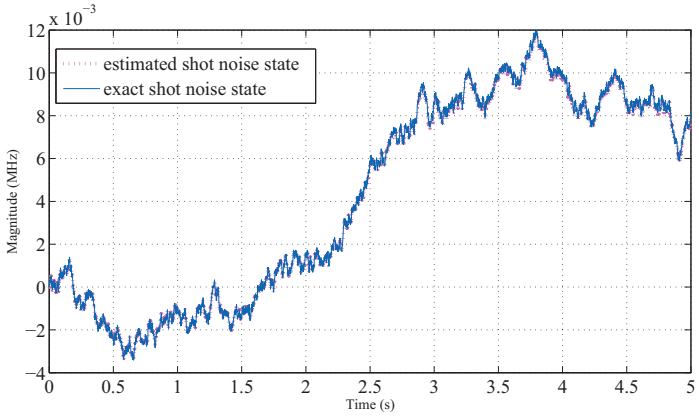

Figure 4.10: Comparison of the estimated and exact shot noise states using the proposed linear controller with the nonlinear system model.

4.3 Key Considerations in Simulations

Remark 4.1 *It is important to note that the quantum system is, in fact, a continuous system, and all sources of noise are also continuous-time signals. However, in the MATLAB/Simulink environment a noise input is modeled as samples of a randomly changing signal. To convert such a discrete-time signal to a realistic noise input, it is required to properly scale the signal by multiplying it by a constant value equal to the second root of the sampling time (see [58] for a detailed description of this mapping from continuous-time to discrete-time).*

It is known that the optimal control law (for a quadratic performance index) for an LTI system is in the form of state feedback. Since the state variables are often not available directly, it is required to use an observer to generate a sufficiently accurate estimate of the state vector first. To this end, one can take advantage of the separation theorem given below for the overall control design [59].

Theorem 4.1 (Separation principle) *Let a stable observer and a stable state feedback be designed for an LTI system. Then the closed-loop system obtained by the combined observer and feedback will be stable. Furthermore, the resultant closed-loop poles consist of the poles of the observer and the poles of the state feedback.*

According to the separation principle described above, the state feedback control design can be treated as two separate problems of designing the feedback gain and the observer gain. The concept of this principle is demonstrated in Fig. 4.11.

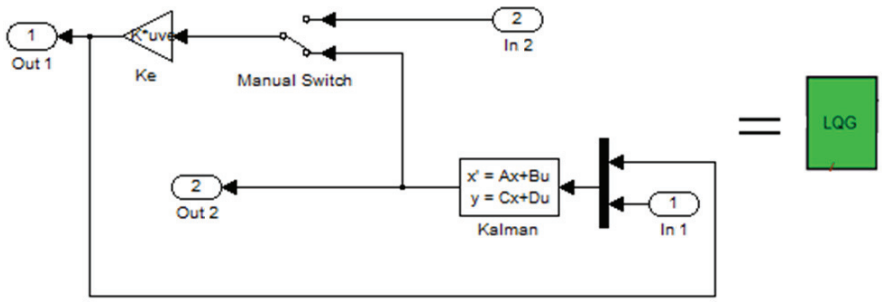

Figure 4.11: Decomposition of LQG control design to the feedback gain design and observer design, using the separation principle.

Remark 4.2 *Usually the poles of the observer are chosen one decade to the left of the state feedback poles for a reasonably fast convergence of the state estimates.*

4.3.1 State estimates

Convergence of state estimates to the exact states is very important in the design of the underlying controller. Using the system parameters given in Table 3.1 with the performance

index as Δ, and placing the poles of the observer one decade to the left of the poles of the state feedback (making the observer dynamics ten times faster than the state feedback), high convergence rate for the state estimation error was observed. In fact, using the observability Gramian it was verified that the integrator state is strongly observable whereas the other state variables (related to the optical amplitude quadrature and shot noise) are less observable.

4.3.2 Numerical error

It was observed by simulation that even with zero initial conditions and in the absence of different noise sources the system output was subject to significant error. This error was numerical, and was effectively suppressed by reducing the default error tolerance level on MATLAB/Simulink to 10^{-8} (the default value was 10^{-3}). The results obtained by default error tolerance and the adjusted value are depicted in Figs. 4.12 and 4.13. The figures show a significant decrease in the error level after reducing the numerical error tolerance using the system parameters given in Table 3.1. Note that the length of the cavity is actuated via a tabular piezoelectric transducer (with a stroke of 10μm when a voltage of 500V is applied).

4.4 Summary

Summarize the main conclusions of this chapter, LQG control method is applied as an efficient approach for a multi-variable system to tackle the problem of mode-squeezing in optomechanical sensors. Coherent feedback quantum control is synthesized by incorporating both shot

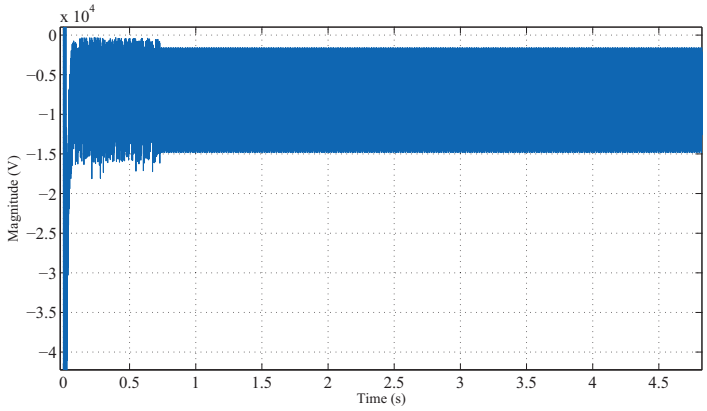

Figure 4.12: Steady-state output with zero initial conditions and in the absence of different noises, before numerical error correction.

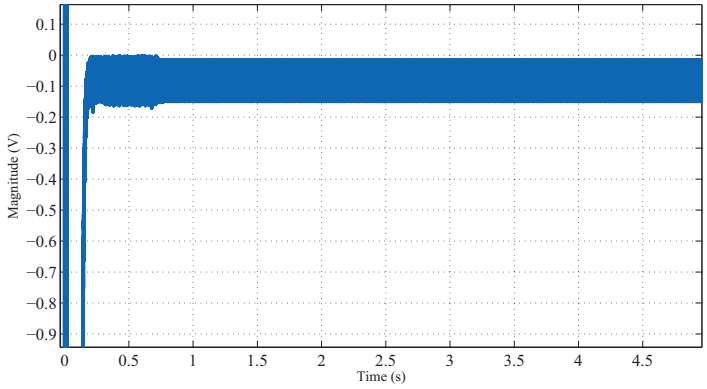

Figure 4.13: Steady-state output with zero initial conditions and in the absence of different noises, after numerical error correction.

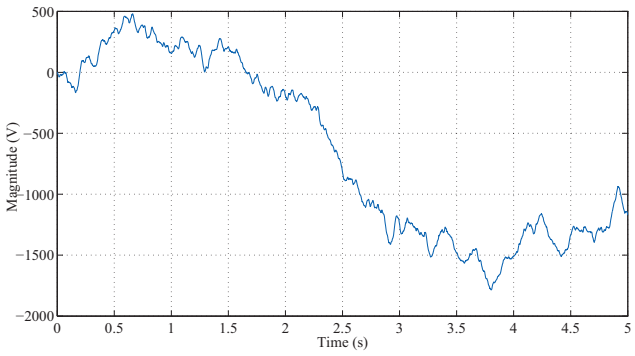

Figure 4.14: Transient response of the control input applied to the piezoelectric transducer.

noise and back-action noise to diminish the output noise well below the shot noise limit. The simulation results show the effectiveness of the proposed control strategy in squeezing the cavity output beam. In the next chapter, it will be shown how to design a reliable and fault tolerant laser system through linear feedback to have robust stability and robust performance features in the sense of real application.

Chapter 5

Robust Controller Design for Optomechanical Sensors

The objective of this chapter is to achieve the robust stabilization and robust performance of the system in practice across critical uncertainties and technical limitations such as laser noise and detector imprecision. This problem is treated as an optimization problem using a non-sampling method called robust H_∞.

5.1 Uncertainty and Robustness

A controller is robust if the closed-loop system response does not violate the desired specifications under parameter perturbations within a sufficiently close neighborhood of the nominal

values. The model may contain parameters whose values are not precisely known. Such parameters vary over a certain range of values (assumed to be known *a priori*), and are referred to as uncertain parameters [60,61]. It is very important in a quantum system like laser cavity that under the designed controller both stability and desired performance are maintained when the system is entangled with different types of uncertainty. It is aimed to use robust control theory to deal with uncertainties in the parameters $\kappa_0, \kappa_1, \kappa_L, \kappa$, and ϕ_{LO} introduced in Chapter 3.

Although usually the emission of laser has a very thin spectral linewidth in the case of single-mode output, it introduces uncertainty in some parameters of the system model such as propagation constant κ. On the other hand, decreasing the linewidth by itself generates quantum noise in the output, which in turn reduces the quality factor Q_0 of the system. These issues need to be taken into account in the design of a robust controller which not only satisfies robustness with respect to parameter uncertainty, but also reduces quantum noise effect and provides some degree of freedom to choose the input power within a sufficiently large range [62].

Homodyne detection plays a key role as an experimental tool in various tests such as position measurement on an atom passing through a standing light wave [63] and the measurements of generalized quasiprobability distributions [64,65]. Homodyne detection schemes are devised to provide the measurement of a single-mode quadrature $X_{\phi_{LO}}$ through the mixing of the cavity output beam signal with a highly excited classical field at the same frequency. This classical field is referred to as the local oscillator [66]. The schematic diagram of a balanced

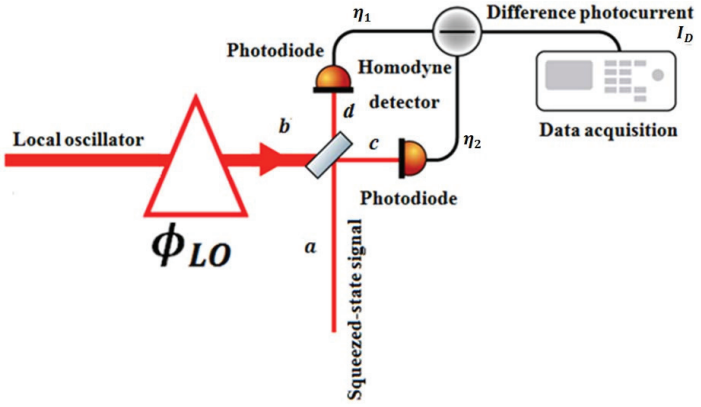

Figure 5.1: Two-port homodyne detector scheme.

homodyne detector is demonstrated in Fig 5.1. The signal mode a interferes with a second mode b excited in a coherent semiclassical state (e.g., a laser beam) in a balanced (50/50) beamsplitter. The mode b is the local oscillator mode of the detector operating at the same frequency as a, and is excited in a coherent state $|z\rangle$ with a relatively large amplitude z. The beamsplitter is tuned to have real coupling, hence no additional phase-shift is imposed on the reflected and transmitted beams. In this case, the local oscillator phase provides a reference for the quadrature measurement, i.e., the phase of the local oscillator is the phase difference between the two modes. After the beamsplitter the two modes are detected by two identical photodetectors (usually linear photodiodes), and finally the difference between the photocurrents at zero frequency is electronically processed and rescaled by $2|z|$. Here, c and d are the

output mode of the beamsplitter. The resulting homodyne photocurrent I_D is given by [66]:

$$\begin{aligned} I_D &= X_{\phi_{LO}} = \frac{(C^\dagger C - d^\dagger d)}{2z} = \frac{(a^\dagger b + b^\dagger a)}{2z} \\ &= \delta X_a cos(\phi_{LO}) + \delta Y_a sin(\phi_{LO}). \end{aligned} \tag{5.1}$$

Note that in (3.10) and (5.1), one can consider $\cos(\phi_{LO})$ and $\sin(\phi_{LO})$ as the uncertain parameters instead of ϕ_{LO}. Note also that the variation of ϕ_{LO} around $\frac{\pi}{2}$ is equal to that of $\cos(\phi_{LO})$ around zero with a good approximation. Fig. 5.2 demonstrates the linear deviation of $\cos(\phi_{LO})$ around $\frac{\pi}{2}$ and no deviation of $\sin(\phi_{LO})$ in that neighborhood.

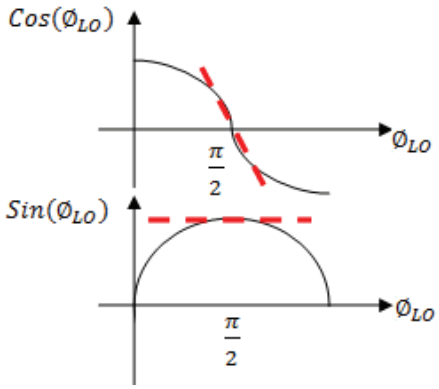

Figure 5.2: Variation of $\cos(\phi_{LO})$ and $\sin(\phi_{LO})$ around $\phi_{LO} = \frac{\pi}{2}$.

The effect of the variation of the decay ratio κ on the squeezing of laser heavily depends on the confinement of laser beam modes inside the cavity (see e.g., [47, 48]). Uncertainty in part of the optical cavity decay parameters is called disturbance attenuation parameter. In

this respect, a maximum deviation of 10% is considered for the optical cavity decay parameters [67].

The objective here is to increase the quantum efficiency of the detector in a feedback-assisted style. The feedback loop is obtained by extracting a fraction of the cavity output which is then processed in order to drive an appropriate actuator acting on the resonator [30]. Beamsplitter is known as the simplest and most efficient way to extract the feedback loop mode [30]. It is desired to achieve the best possible squeezing of the output mode. In order to squeeze the light beam, it is crucial that the noise level does not exceed the shot noise limit [30]. By changing the local oscillator phase, one can manipulate two output states. As such, since this application requires squeezed phase quadrature state, one has to fix ϕ_{LO} at $\frac{\pi}{2}$ through a schematic called *90-degree optical hybrid* [68] as it is shown in Fig. 5.1. Uncertainty in part of the homodyne detector, namely non-unit quantum efficiency of detectors ϕ_{LO}, is originated from:

- Impurity of beamsplitter.
- ϕ_{LO} may not be exactly adjusted at the best sensitivity working point all the time, and is shifted by $\frac{\pi}{2}$ after every couple of measurements leading to cumulative diffraction from $\frac{\pi}{2}$ [69].

Since the system here is a feedback mediated process, many desired output properties can be achieved by proper design. In particular, by an appropriate robust control design approach, there is no need to use:

- A phase shifter (phase compensator) in front of the beamsplitter.
- The same laser source for both local oscillator and laser beam [64].

It is to be noted that here a preamplifier is used before the homodyne detector to amplify the cavity output beam signal but the drawback of this method is that the existing noise will also be amplified, which is undesirable [64]. One can use H_∞ control design technique to address this drawback to some extent.

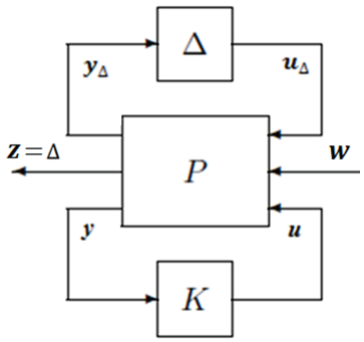

Figure 5.3: Multiplicatively perturbed feedback system with Δ pulled off.

Fig. 5.3 shows the linear fractional transformation (LFT) representation of the multiplicatively perturbed feedback system with Δ pulled off. A necessary and sufficient condition is provided in the next theorem (known as the *small gain theorem* [70]) for the well-posedness and internal stability of the system under an H_∞ controller which is aimed to minimize the effect of disturbance w in the output.

Definition 5.1 ($\Re H_\infty$ *space*) *The real rational subspace of* H_∞*, which consists of all strictly proper and real rational stable transfer function matrices, is denoted by* $\Re H_\infty$ *[71].*

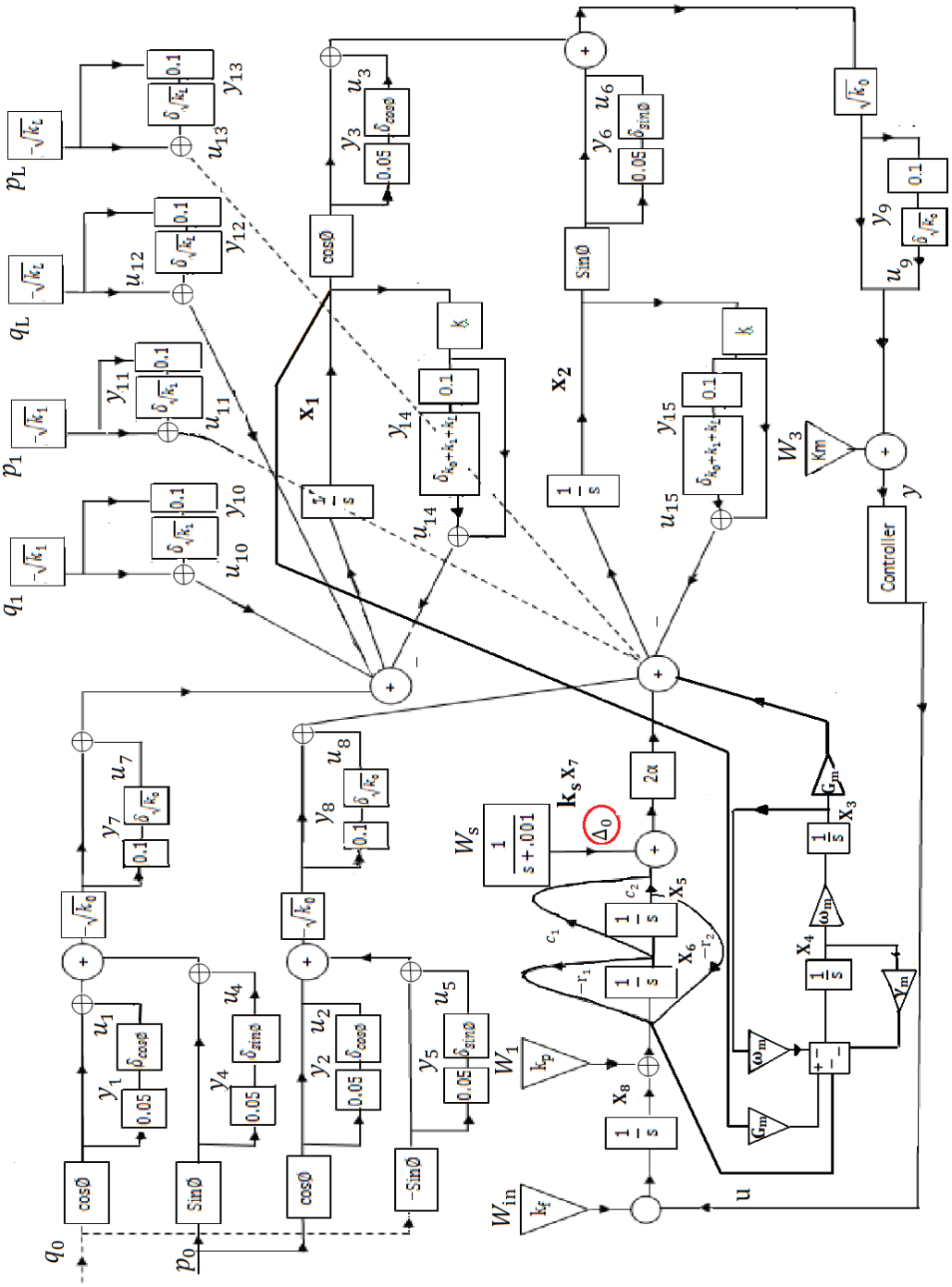

Figure 5.4: Large-scale view of multiplicatively perturbed feedback system with Δs from their respective points.

Theorem 5.1 (Small Gain Theorem) *Given $P \in \Re H_\infty$, the interconnected system of Fig. 5.3 is well-posed and internally stable for all $\Delta(s) \in \Re H_\infty$ with $\|\Delta\|_\infty \leq \frac{1}{\gamma}$ if and only if $\|P(s)\|_\infty \leq \gamma$, for $\gamma > 0$ [70].*

This can be described as [71]:

$$\|T_{zw}\|_\infty \triangleq \sup_\omega \sigma_{max}(T_{zw}(j\omega)) < \gamma \tag{5.2a}$$

$$CL = F_\ell(P,K). \tag{5.2b}$$

where $F_\ell(P,K)$ represents the lower LFT synthesis of the plant P and the controller K, and T_{zw} is the transfer function matrix from the disturbance w to the output z, and $||.||_\infty$ denotes the infinity norm [70, 72]. Fig. 5.4 shows Large-scale view of the multiplicatively perturbed feedback plant with Δs from their respective points.

In order to design an H_∞ controller, the plant is required to be stabilizable from the control input $\tilde{u}$ and detectable from the measurement output y. One can partition the plant P given in Fig. 5.3 in the state space as follows:

$$\left[\begin{array}{c|cc} A & B_1 & B_2 \\ \hline C_1 & D_{11} & D_{12} \\ C_2 & D_{21} & D_{22} \end{array}\right]$$

Here the input channels B_1 and B_2 correspond to the disturbance and control input, respectively. Also, the output channels C_1 and C_2 generate the errors (which are desired to be maintained small) and the output measurements (provided to the controller), respectively. $D = (D_{11}, D_{12}; D_{21}, D_{22})$ is the feedthrough (or feedforward) matrix. The controller K stabilizes the plant P (and has the same number of states as P) if $(A, B2)$ is stabilizable and $(C2, A)$ is detectable [71].

Remark 5.1 *The robust H_∞ synthesis in MATLAB uses the Hinfsyn algorithm. This algorithm works best when the following conditions are satisfied by the plant [73]:*

- $D12$ *and* $D21$ *are full-rank;*
- $\begin{bmatrix} A - j\omega I & B_2 \\ C_1 & D_{12} \end{bmatrix}$ *has full column rank for* $\omega \in R$, *and*
- $\begin{bmatrix} A - j\omega I & B_1 \\ C_2 & D_{21} \end{bmatrix}$ *has full column rank for* $\omega \in R$.

In the current plant D_{12} is not full-rank due to the nature of the corresponding quantum system. This can result in an H_∞ controller that has a large high-frequency gain.

The value of γ as an output argument in Hinfsyn algorithm is relatively large for the present system because the optical coupling κ is much larger than the optomechanical coupling G_0, which leads to a high condition number for the system matrix.

As mentioned earlier, for the purpose of tracking, an integrator is placed in series with the plant and the controller is designed for the combined system. However, in the H_∞ analysis,

one may consider $1/(s+\varepsilon)$ instead of $1/s$ which is inclusively taken into account in Hinfsyn algorithm in MATLAB [73] (this is mainly for the stability purpose). It is important to note that the controller designed by H_∞ method does not guarantee the closed-loop stability. It is shown in the next section that the designed controller stabilizes the closed-loop system in a sufficiently small neighborhood of the nominal operating point.

5.2 Robust Stabilizability vs. Robust Performance

The uncertainty in the plant can be modeled by a polynomial expression [74]. For the controller design, robust stabilizability has higher priority than robust performance. Using the information available about the structure of any part of the system, one can come up with the balance in the trade off between robust stabilizability and robust performance for designing a cost-effective controller. The two uncertainty terms $\cos(\phi_{LO})$ and $\sin(\phi_{LO})$ are correlated according to the Pythagorean theorem. To simplify the controller design, one can take into account the range of variation of the uncertain parameters $\delta\cos(\phi_{LO})$ and $\delta\sin(\phi_{LO})$. This point is demonstrated in Fig. 5.5. This leads to a less conservative control scheme. It was shown in [75] that if the system with polynomial uncertainty is stabilizable at some points in the given region, then it is also stabilizable at any point in the region, as long as those points do not lie on a specific algebraic variety. This means that if the nominal model of the system is stabilizable, so is the system at almost all operating points. The H_∞ algorithm was

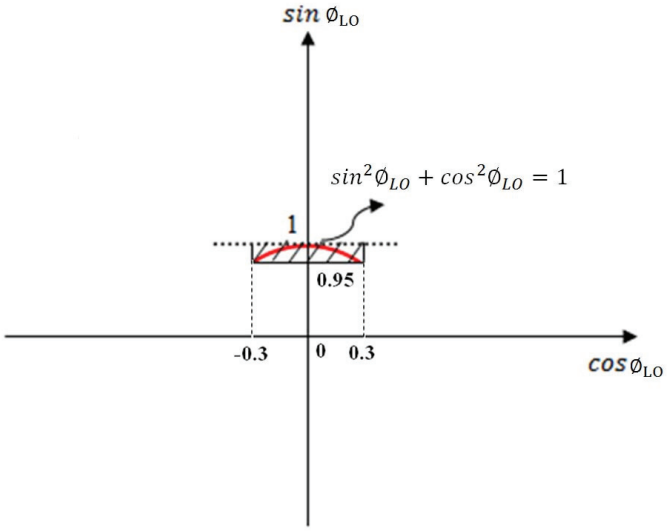

Figure 5.5: The region of uncertainty for the parameters $\sin(\phi_{LO})$ and $\cos(\phi_{LO})$ around the nominal point $\phi_{LO} = \frac{\pi}{2}$.

tested randomly for different deviations of $\delta\cos(\phi_{LO})$ and $\delta\sin(\phi_{LO})$ in the corresponding region (shown in Fig. 5.5). For 1000 randomly selected points in the interval associated with $\delta\cos(\phi_{LO}) > 0.3$ and $\delta\sin(\phi_{LO}) > 0.05$ it was shown by simulation that in less than 1% of the cases the resultant closed-loop system was unstable as shown in Fig. 5.6. In this figure, an H_∞ controller is designed to deal with the uncertain system, where 30% deviation is considered in ϕ_{LO} corresponding to each single point. Simulation is performed with 1000 randomly selected points for ϕ_{LO} in the interval between the specified point and the nominal point $\phi_{LO} = \frac{\pi}{2}$, and the percentage of unstable closed-loop systems is recorded. Fig. 5.7 shows that the output Δ has its least H_∞ performance error value at $\phi_{LO} = \frac{\pi}{2}$, as expected. Figures 5.8 and 5.9 illustrate the Δ performance for the linearized and nonlinear models, respectively, while ϕ_{LO}

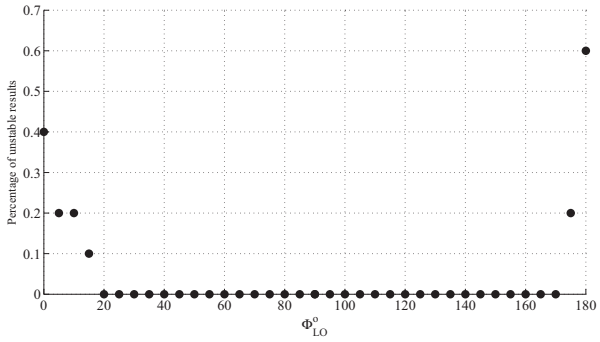

Figure 5.6: Percentage of cases where the closed-loop system corresponding to 1000 randomly selected parameters in the uncertain region around the nominal point $\phi_{LO} = \frac{\pi}{2}$ is unstable with a fixed H_∞ controller designed for 30% deviation in ϕ_{LO}.

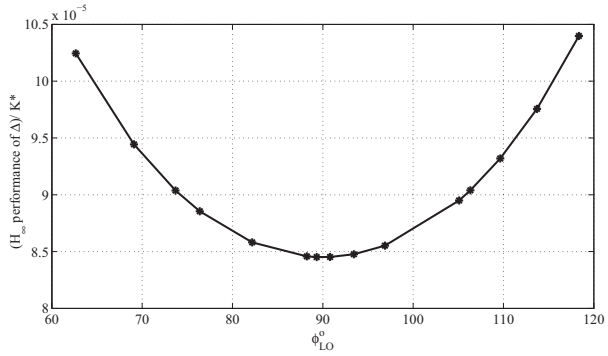

Figure 5.7: The resultant H_∞ performance for different values of the uncertain parameter ϕ_{LO}.

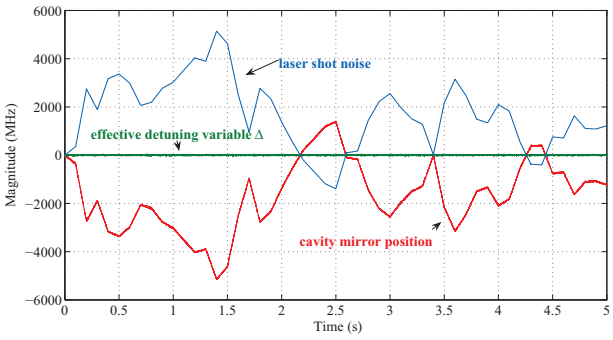

Figure 5.8: The output Δ and its components for the closed-loop system with linearized model and 30% deviation in ϕ_{LO}.

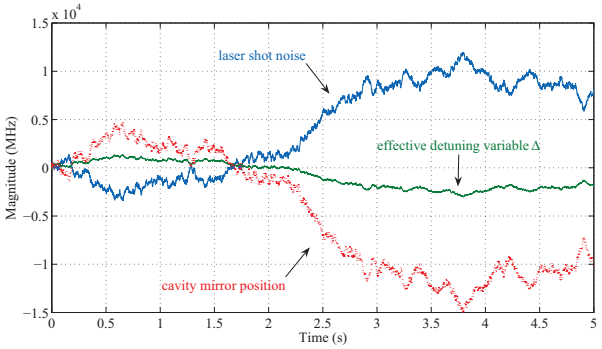

Figure 5.9: The output Δ and its components for the closed-loop system with the original nonlinear model and 30% deviation in ϕ_{LO}.

is perturbed by 30% from its nominal point $\frac{\pi}{2}$. It is evident that the system is stabilized under the designed H_∞ controller, but the tracking error is not completely regulated to zero in the nonlinear model, which was expected from the control structure.

5.3 Summary

Summarized in a further report, a complete LFT representation of the system is provided in the presence of different terms of uncertainty and detector imprecisions. Thereafter, robust H_∞ method is employed to guarantee the robust stabilization and robust performance of the system in practice. Without loss of generality, having taken advantage of the existent structural correlation among the parameters, the given design yields to be not conservative and its results demonstrate a reasonable performance in front of nonlinear model.

Chapter 6

Conclusions and Future Work

6.1 Summary of Contributions

In this work, a linear quadratic Gaussian (LQG) controller is designed for laser squeezing in an optomechanical system. A model is developed first in Chapter 3, that takes into account all sources of noise which are often neglected in existing work to simplify the problem. Since the model includes nonlinear terms, it is linearized around a suitable operating point in order to be able to use the LQG control framework. A proper cost function is used in Chapter 4 to reflect the fluctuation of the amplitude quadrature of the fundamental output field. The performance of the controller is verified via simulation by applying it to the original nonlinear model. The results confirm that the squeezing objective is achieved for the realistic noise levels used in simulations. Furthermore, using the H_∞ control design technique in Chapter 5, the quantum

system is stabilized in the presence of model mismatches and disturbances. To summarize the contribution of this work:

- A nonlinear model of quantum optomechanical sensors is considered first, with various sources of noise.
- Control techniques are employed in order to:
  - Achieve frequency locking of laser cavity for the case of optomechanical sensors using an optimal servo controller.
  - Improve stability and increase the measurement efficiency of quantum optics systems using an H_∞ controller.

The results of this work can be used to implement controllers with robust performance lasers with fluctuations approaching the quantum noise limit. The resultant controller can be used in a wide range of high-precision laser applications.

6.2 Suggestions for Future Work

Quantum control is still in its infancy. The research presented in this thesis provides a foundation for future research in the field of quantum feedback control, where it is desired to design a reliable and fault tolerant laser system through linear feedback. Some relevant open questions are: How does a weak measurement [76] affect quantum systems under feedback control? To

what extent is it possible to control nonlinear dynamics of quantum systems using linear controllers? What approaches are effective for control of quantum systems with non-Markovian dynamics [77–79]? What are the limitations of feedback control in dealing with uncertainties in quantum systems? How can one synthesize complex quantum feedback network systems? These questions (and many more) are some of the problems which can be addressed in the future.

Bibliography

[1] M. Chester, *Primer of Quantum Mechanics*. New York: John Wiley, 1987.

[2] R. Feynman, *The Strange Theory of Light and Matter*. Princeton: Princeton University Press, 1985.

[3] D. J. Griffiths, *Introduction to Quantum Mechanics*. US: Pearson, 2004.

[4] S. Chu, "Cold atoms and quantum control," *Nature*, vol. 416, 2002.

[5] M. Dantus and V. Lozovoy, "Experimental coherent laser control of physicochemical processes," *Chem. Reviews*, vol. 104, 2004.

[6] H. Rabitz, R. d. Vivie-Riedle, M. Motzkus, and K. Kompa, "Whither the future of controlling quantum phenomena?," *Science*, vol. 288, no. 5467, pp. 824–828, 2000.

[7] L. Accardi, Y. Lu, and I. Volovich, *Quantum Theory and Its Stochastic Limit*. New York: Springer Verlag, 2002.

[8] P. H. Breuer and F. Petruccione, *The Theory of Open Quantum Systems*. Oxford: Oxford University Press, 2007.

[9] N. Khaneja, R. Brockett, and S. J. Glaser, "Time-optimal control of two-spin systems," *Phys. Rev. A*, vol. 63, 2001.

[10] D. Sugny, C. Kontz, and H. R. Jauslin, "Time-optimal control of a two-level dissipative quantum system," *Phys. Rev. A*, vol. 76, 2007.

[11] D. D. 'Alessandro and M. Dahleh, "Optimal control of two-level quantum systems," *IEEE Transactions on Automatic Control*, vol. 46, no. 6, 2001.

[12] S. Grivopoulos and B. Bamieh, "Optimal population transfers in a quantum system for large transfer time," *IEEE Transactions on Automatic Control*, vol. 53, no. 4, 2008.

[13] S. Z. S. Hassen, M. Heurs, E. H. Huntington, I. R. Peterson, and M. R. James, "Frequency locking of an optical cavity using linear-quadratic gaussian integral control," *Phys. B: At. Mol. Opt. Phys.*, vol. 42, no. 17, p. 175501, 2009.

[14] R. V. Pound, "Electronic frequency stabilization of microwave oscillators," *Review of Scientific Instruments*, vol. 17, no. 11, pp. 490–505, 1946.

[15] T. W. Hansch and B. Couillaud, "Laser frequency stabilization by polarization spectroscopy of a reflecting reference cavity," *Optics communications*, vol. 35, no. 3, pp. 441–444, 1980.

[16] M. M. Wronski, *Development of a flat panel detector with avalanche gain for Interventional Radiology*. PhD thesis, University of Toronto.

[17] Y. Yamamoto, O. Nilsson, and S. Machida, "Amplitude squeezing in a pump-noise-suppressed laser oscillator," *Phys. Rev. A*, vol. 34, no. 5, 1986.

[18] C. Genes, A. Mari, D. Vitali, and P. Tombesi, "Quantum effects in optomechanical systems," *Adv. At. Mol. Opt. Phys.*, vol. 57, 2009.

[19] T. J. Kippenberg and K. J. Vahala, "Cavity opto-mechanics," *Optics Express*, vol. 15, no. 25, pp. 17172–17205, 2007.

[20] E. D. Black, "An introduction to pound-drever-hall laser frequency stabilization," *Am. J. Phys.*, vol. 69, no. 1, pp. 79–87, 2001.

[21] M. A. Nielsen and I. L. Chuang, *Quantum Computation and Quantum Information*. Cambridge, England: Cambridge University Press, Cambridge, England, 1st ed., 2000.

[22] I. Teper, G. Vrijsen, J. Lee, and M. A. Kasevich, "Backaction noise produced via cavity-aided nondemolition measurement of an atomic clock state," *Phys. Rev. A*, vol. 78, no. 5, 2008.

[23] M. Thorpe, K. Moll, R. J. Jones, and B. Safdi, "Broadband cavity ringdown spectroscopy for sensitive and rapid molecular detection," *Science*, vol. 311, no. 5767, 2006.

[24] M. Thorpe, K. Moll, R. J. Jones, and B. Safdi, "Precise measurements of optical cavity dispersion and mirror coating properties via femtosecondcombs," *Optics Express*, vol. 13, no. 3, 2005.

[25] C. M. Caves, "Precise measurements of optical cavity dispersion and mirror coating properties via femtosecondcombs," *Phys. Rev. D*, vol. 26, no. 8, 1982.

[26] D. Walls, "Precise measurements of optical cavity dispersion and mirror coating properties via femtosecondcombs," *Nature*, vol. 306, 1983.

[27] A. A. Clerk, F. Marquardt, and K. Jacobs, "Back-action evasion and squeezing of a mechanical resonator using a cavity detector," *New J. Phys*, vol. 10, no. 095010, 2008.

[28] M. Tsang and C. M. Caves, "Coherent quantum-noise cancellation for optomechanical sensors," *Phys Rev Lett.*, vol. 105, no. 12, 2010.

[29] V. B. Braginsky and F. Y. Khalili, *Quantum Measurement*. Cambridge, England: Cambridge University Press, 1992.

[30] D. Vitali and P. Tombesi, "Feedback-assisted ponderomotive squeezing," *C. R. Physique. doi:10.1016/j. crhy. 2010.12.007*, 2011.

[31] D. Dong and I. Petersen, "Quantum control theory and applications: A survey," *IET Control Theory & Applications*, vol. 4, no. 12, pp. 2651–2671, 2010.

[32] M. Mirrahimi, P. Rouchon, and G. Turinici, "Lyapunov control of bilinear schrödinger equations," *Automatica*, vol. 41, 2005.

[33] S. Kuang and S. Cong, "Lyapunov control methods of closed quantum systems," *Automatica*, vol. 44, 2008.

[34] A. Ferrante, M. Pavon, and G. Raccanelli, "Driving the propagator of a spin system: a feedback approach," in *Proceedings of the 41st IEEE Conference on Decision and Control*, (Las Vegas, NV, USA), 2002.

[35] R. A. Serway, J. W. Jewett, and T. C. Ralph, *Physics for Scientists and Engineers*. Brooks Cole, 2003.

[36] D. Simon, *Optimal state estimation: Kalman, H [infinity] and nonlinear approaches*. John Wiley and Sons, 2006.

[37] E. H. Huntington, C. Harb, M. Heurs, and T. C. Ralph, "Signal-to-noise ratio of preamplified homodyne detection in quantum tomography," *Phys. Rev. A*, vol. 75, no. 013802, 2007.

[38] S. O. Kasap, *Optoelectronics and Photonics*. Prentice Hall, 2001.

[39] R. A. Baumgartner and R. L. Byer, "Optical parametric amplification," *IEEE Quantum Electron*, vol. QE-15, no. 6, p. 432, 1979.

[40] R. L. Byer and A. Piskarskas, "Feature issue on optical parametric oscillation and amplification," *Opt. Soc. Am. B*, vol. 10, no. 9, p. 2148, 1993.

[41] G. Arisholm, R. Paschotta, and T. Südmeyer, "Limits to the power scalability of high-gain optical parametric oscillators and amplifiers," *Opt. Soc. Am. B*, vol. 21, no. 3, p. 578, 2004.

[42] G. Cerulla and C. Manzoni, *Solid-state ultrafast optical parametric amplifiers*. Solid-State Lasers and Applications/CRC Press, 2007.

[43] MIT Open Course Ware: MIT Understanding lasers and fiber optics, "Laser fundamentals III."

[44] C. W. Gardiner and P. Zoller, *Quantum Noise*. Berlin: Springer, 2000.

[45] M. Aspelmeyer, S. Groblacher, K. Hammerer, and N. Kiesel, "Quantum optomechanics-throwing a glance," *Opt. Soc. Ame. B*, vol. 27, no. 6, p. A189, 2010.

[46] S. Z. S. Hassen and I. R. Petersen, "A time-varying kalman filter approach to integral LQG frequency locking of an optical cavity," in *Proceedings of the American Control Conference*, (Baltimore, MD, USA), pp. 2736–2741, June 2010.

[47] T. K. Boyson, T. G. Spence, M. E. Calzada, and C. C. Harb, "Frequency domain analysis for laser-locked cavity ringdown spectroscopy," *Optics Express*, vol. 19, no. 9, 2011.

[48] A. G. Kallapur, I. R. Petersen, T. K. Boyson, and C. C. Harb, "Nonlinear estimation of a fabry-perot optical cavity for cavity ring-down spectroscopy," in *Proceedings of 2010 IEEE International Conference on Control Applications*, (Yokohama, Japan), pp. 298–303, September 2010.

[49] M. Salehizadeh, J. Habibi, A. G. Aghdam, and M. Z. Kabir, "Laser cavity squeezing using optimal servo controller in optomechanical sensors," submitted to a conference.

[50] A. Dorsel, J. D. McCullen, P. Meystre, E. Vignes, and H. Walther, "Optical bistability and mirror confinement induced by radiation pressure," *Phys. Rev.*, vol. 51, no. 013802, pp. 1550–1553, 1983.

[51] H. A. Bachor and T. C. Ralph, *A Guide to Experiments in Quantum Optics*. Wiley-VCH Verlag, 2004.

[52] S. Z. S. Hassen, I. R. Petersen, E. H. Huntington, M. Heurs, and M. R. James, "LQG control of an optical squeezer," in *Proceedings of American Control Conference*, (Baltimore, MD, USA), pp. 2730–2735, June 2010.

[53] M. A. Marchiolli, S. S. Mizrahi, and V. V. Dodonov, "Signal-to-noise ratio of preamplified homodyne detection in quantum tomography," *Phys. Rev. A*, vol. 57, no. 5, 1998.

[54] E. H. Huntington, M. R. James, and I. R. Peterson, "Laser-cavity frequency locking using modern control," in *Proceedings of 46th IEEE conference on Decision and Control*, (New Orleans, LA, USA), pp. 6346–6351, December 2007.

[55] H. Kwakernaak and R. Sivan, *Linear optimal control systems*. Newyork: Wiley, 1972.

[56] G. F. Franklin, J. D. Powell, and M. L. Workman, *Digital Control of Dynamic Systems*. Berlin: Addison-Wesley, 1998.

[57] M. J. Grimble, "Design of optimal stochastic regulating systems including integral action," *Proc. IEEE Control & Science*, vol. 126, no. 9, pp. 841–848, 1979.

[58] D. D. Sworder and J. E. Boyd, *Estimation problems in hybrid systems*. Cambridge: Cambridge University Press, 1999.

[59] C. Brezinski, *omputational Aspects of Linear Control (Numerical Methods and Algorithms)*. Cambridge: Springer, 2002.

[60] H. Zhang and H. Rabitz, "Robust optimal control of quantum molecular systems in the presence of disturbances and uncertainties," *Phys. Rev. A*, vol. 49, no. 4, pp. 2241–2254, 1994.

[61] H. Rabitz, "Optimal control of quantum systems: Origins of inherent robustness to control field fluctuations," *Phys. Rev. A*, vol. 66, no. 6, 2002.

[62] C. H. Henry, "Theory of the linewidth of semiconductor lasers," *IEEE Quantum Electron*, vol. 18, no. 2, p. 259, 1982.

[63] P. Storey, M. Collett, and D. Walls, "Atomic-position resolution by quadrature-field measurement," *Phys. Rev. A*, vol. 47, 1993.

[64] U. Leonhardt and H. Paul, "High-accuracy optical homodyne detection with low-effciency detectors: Preamplification from antisqueezing," *Phys Rev Lett.*, vol. 72, no. 26, 1994.

[65] N. G. Walker, "Quantum theory of multiport optical homodyning," *Modern Optics*, vol. 34, no. 1, pp. 15–60, 1987.

[66] A. Ferraro, S. Olivares, and M. G. A. Paris, *Gaussian states in continuous variable quantum information*. Lecture notes in Quantum Optics and Quantum Information given by one of us (MGAP) at the University of Napoli and the University of Milano.

[67] M. R. James, H. I. Nurdin, and I. R. Petersen, "H_∞ control of linear quantum stochastic systems," *Quantum-Atom Optics Downunder, OSA Technical Digest*, 2007.

[68] H. Y. Choi, Y. Takushima, and Y. C. Chung, "Optical performance monitoring technique using asynchronous amplitude and phase histograms," *Optics Express*, vol. 17, no. 26, pp. 23953–23958, 2009.

[69] G. M. D. 'Ariano, M. G. A. Paris, and R. Seno, "Feedback-assisted homodyne detection of phase shifts," *Physical Review A*, vol. 54, no. 5, pp. 4495–4504, 1996.

[70] K. Zhou and J. C. Doyle, *Essentials of robust control*. Prentice Hall, 1999.

[71] K. Glover and J. Doyle, "State-space formulae for all stabilizing controllers that satisfy an H_∞ norm bound and relations to risk sensitivity," *Systems and Control Letters*, vol. 11, pp. 167–172, 1988.

[72] J. C. Doyle, B. Francis, and A. Tannenbaum, *Feedback control theory*. Macmillan Publishing Co., 1990.

[73] Robust Control Theory Toolbox, Matlab.

[74] J. Fisher and R. Bhattacharya, "On stochastic LQR design and polynomial chaos," in *Proceedings of the American Control Conference*, (Seattle, WA, USA), pp. 95–100, June 2008.

[75] S. Sojoudi, J. Lavaei, and A. G. Aghdam, "Robust stabilizability verification of polynomially uncertain LTI systems," *IEEE Transactions on Automatic Control*, vol. 52, no. 9, 2007.

[76] S. Lloyd, J. Jacques, and E. Slotine, "Quantum feedback with weak measurements," *Phys. Rev. A*, vol. 62, no. 1, 2000.

[77] V. Giovannetti, P. Tombesi, and D. Vitali, "Non-markovian quantum feedback from homodyne measurements: The effect of a nonzero feedback delay time," *Phys. Rev. A*, vol. 60, no. 1, 1999.

[78] J. Wang, H. M. Wiseman, and G. J. Milburn, "Non-markovian homodyne-mediated feedback on a two-level atom: A quantum trajectory treatment," *Chem. Phys.*, vol. 268, 2001.

[79] W. Cui, Z. R. Xi, and Y. Pan, "Optimal decoherence control in non-markovian open dissipative quantum systems," *Phys. Rev. A*, vol. 77, no. 3, 2008.

Appendix A

Appendix

A.1 MATLAB Codes

The simulations in this thesis are performed using MATLAB version 7.2.0.232 (*R*2006*a*) Service Pack 2 from Mathworks. The main MATLAB codes used in this project are provided in this appendix.

A.1.1 Controller design

```
%%%   Optical cavity model   %%%

%%%%  DataBase   %%%%

plant=ss(A,B,C,D);

%% Design the regulator by computing the LQR Gain matrix K

[Ke,S,e]=lqr(A, B, Qn, R);
```

```
%% Compute the Kalman filter gains

P1 = ss(A, [B G], C, [D H]);

[Observer, Ko] = kalman(P1, Rw, Rv,[]);

%% Create the regulator and the closed-loop system

lqg_reg = lqgreg(Observer, Ke);

feedin = [1];      % force u

feedout = [1];     % y

Gcl = feedback(plant*lqg_reg, 1, feedin, feedout, +1);

bode(lqg_reg);
```

A.1.2 Robustness design

```
%%%   Robustness  Study   %%%

MatM=funval(Alpha,Dcos,Dk,Dsin,Dsqrtk0,Dsqrtk1,DsqrtkL,Gamma,Gm,...

Osp,c1,c2,eps4,k,k0,k1,k2,kL,kf,km,kp,ks,phi,r1,r2,wm);

A=MatM(1:8,1:8);

B=MatM(1:8,9:35);

C=MatM(9:25,1:8);

D=MatM(9:25,9:35);

sys=ss(A,B,C,D);

[KK,CL,GAM,INFO] = hinfsyn(sys,1,1,'DISPLAY','on');
```